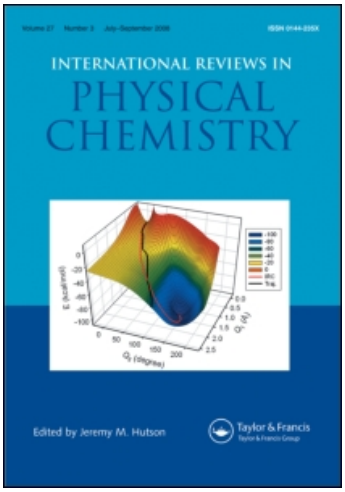

International Reviews in Physical Chemistry
Publication details, including instructions for authors and subscription information:
http://www.informaworld.com/smpp/title~content=t713724383

Mechanism of charge transport in self-organizing organic materials

Ferdinand C. Grozema[a]; Laurens D. A. Siebbeles[a]
[a] Opto-electronic Materials Section, DelftChemTech, Delft University of Technology, Julianalaan 136, 2628 BL, Delft, The Netherlands

To cite this Article Grozema, Ferdinand C. and Siebbeles, Laurens D. A.(2008) 'Mechanism of charge transport in self-organizing organic materials', International Reviews in Physical Chemistry, 27: 1, 87 — 138
To link to this Article: DOI: 10.1080/01442350701782776
URL: http://dx.doi.org/10.1080/01442350701782776

International Reviews in Physical Chemistry
Vol. 27, No. 1, January–March 2008, 87–138

Taylor & Francis
Taylor & Francis Group

Mechanism of charge transport in self-organizing organic materials

Ferdinand C. Grozema and Laurens D.A. Siebbeles*

Opto-electronic Materials Section, DelftChemTech, Delft University of Technology, Julianalaan 136, 2628 BL, Delft, The Netherlands

(*Received 14 September 2007; final version received 31 October 2007*)

Currently there is great interest in the use of organic materials as the active component in opto-electronic devices such as field-effect transistors, light-emitting diodes, solar cells and in nanoscale molecular electronics. Device performance is to a large extent determined by the mobility of charge carriers, which strongly depends on material morphology. Therefore, a fundamental understanding of the relation between the mechanism of charge transport and chemical composition and supramolecular organization of the active organic material is essential for improvement of device performance. Self-assembling materials are of specific interest, since they have the potential to form well defined structures in which molecular ordering facilitates efficient charge transport. This review gives an overview of theoretical models that can be used to describe the mobility of charge carriers, including band theory for structurally ordered materials, tight-binding models for weakly disordered systems and hopping models for localized charges in strongly disordered materials. It is discussed how the charge transport parameters needed in these models; *i.e.* charge transfer integrals, site energies and reorganization energies, can be obtained from quantum chemical calculations. Illustrative examples of application of the theoretical methods to charge transport in self-assembling materials are discussed: columns of discotic molecules, stacks of oligo(phenylene-vinylene) molecules and strands of DNA base pairs. It is argued that the mobility of charge carriers along stacks of triphenylene and oligo(phenylene-vinylene) molecules can be significantly enhanced by improvement of molecular organization. According to calculations, the mobility of charge carriers along DNA strands is strongly limited by the large charge induced structural reorganization of the nucleobases and the surrounding water.

Keywords: charge carrier mobility; discotic molecules; DNA; organic semiconductors; self-assembling systems; theory

Contents

*Corresponding author. Email: l.d.a.siebbeles@tudelft.nl

ISSN 0144–235X print/ISSN 1366–591X online

DOI: 10.1080/01442350701782776
http://www.informaworld.com

1. Introduction

Organic semiconductors are promising materials for use as the active layer in opto-electronic devices[1–3] such as field-effect transistors (FET),[3–6] light-emitting diodes (LEDs)[3,7] and photovoltaic cells.[2,3,8–15] Most organic semiconductors are based on π-conjugated molecules, ranging in size from small molecules to polymers.[16] Important advantages of using organic materials rather than inorganic semiconductors are the relatively low production and processing costs, their flexibility and a low weight. Organic semiconductors can often be processed from solution, using techniques such as spin coating or ink-jet printing. This makes them considerably cheaper to process than inorganic semiconductors, for which high temperatures and ultraclean high-vacuum conditions are necessary. The low cost, together with the low weight and flexibility opens the way to the production of cheap flexible disposable electronics such as smart radio-frequency identity tags to mark products in shops or luggage at airports.[17,18] Organic FETs, LEDs and solar cells will lead to new applications including flexible displays or solar panels, with the active organic component possibly being deposited as paint.

Another important advantage of using organic materials is that their properties, such as their colour or the ionization potential (work function), can be tailored by variations in the molecular structure; *e.g.* changing the degree of conjugation in the polymer or by introduction of electronically active substituents.[19,20] The organization of the individual molecules on a supramolecular level is also known to have a pronounced effect on the opto-electronic properties of the material in the solid state.[21] Stacking of π-conjugated molecules has important consequences for the absorption spectrum of the material and often the fluorescence efficiency is very different in the solid than for the same molecule in solution.[21]

In devices such as FETs, LEDs and photovoltaic cells, charges need to move between the electrodes and, consequently, the mobility of charge carriers is one of the key parameters that determines device performance. The charge carrier mobility, μ, determines the drift-speed, v_d, of charges when an external electric field, E_0, is applied, according to

$$v_d = \mu E_0. \quad (1)$$

Typical electrode distances in devices are tens to hundreds of nanometres. Hence, charge transport in devices invariably involves transfer between a large number of molecules. A high rate of charge transport between molecules in the material is thus essential to achieve good device characteristics. Improved ordering of organic semiconductors on a molecular scale can significantly enhance the electronic interactions between molecular units, which in turn leads to a higher charge carrier mobility. The highest charge carrier mobilities from DC current measurements on devices (FETs) are generally obtained for highly ordered aromatic molecular crystals.[22] Some examples of chemical structures of the molecules in these crystals are shown in Figure 1.

The oligoacenes tetracene and pentacene are among the most studied organic semiconductors and very high charge carrier mobilities have been reported. The mobility values for tetracene and pentacene have gradually increased over the last two decades with

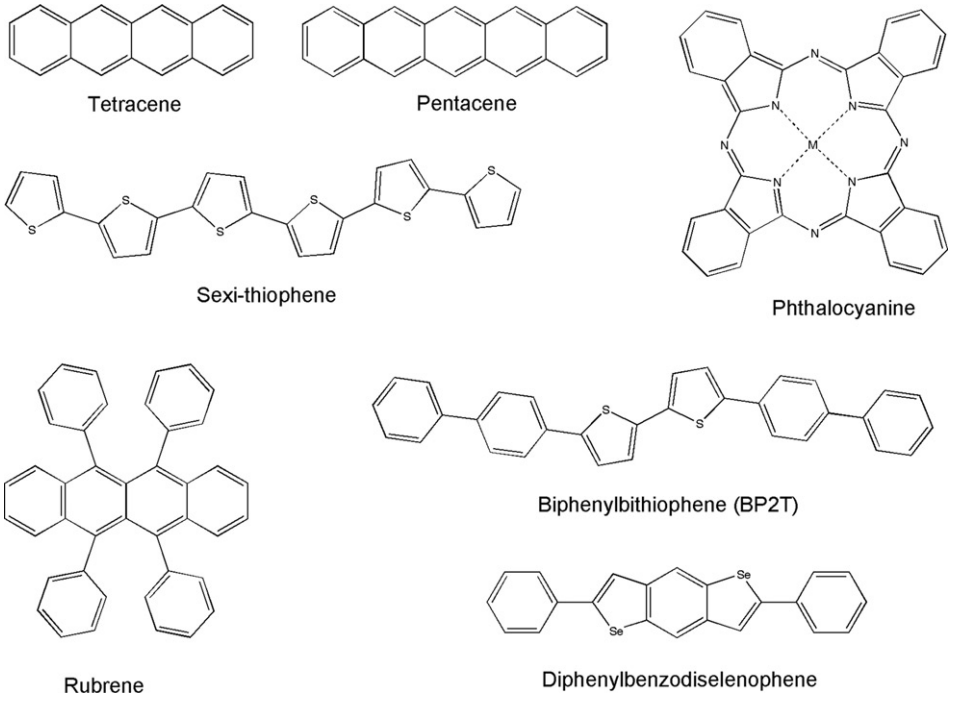

Figure 1. Examples of conjugated molecules that form highly ordered molecular crystals when deposited from vacuum.

the highest reported values to date being[23,24] $2.4\,cm^2\,V^{-1}\,s^{-1}$ and[25] $35\,cm^2\,V^{-1}\,s^{-1}$, respectively. The reason for the increasing mobility over the years is the improved purity of the materials. Even though the single crystalline materials are inherently very pure, the presence of trace amounts of impurities has a detrimental effect on the mobility measured in FET devices.[25] Rubrene is a tetracene derivative that has received a great deal of attention recently, since a very high mobility[26,27] ($20\,cm^2\,V^{-1}\,s^{-1}$) has been measured for crystals of this material. For the other materials shown in Figure 1 mobilities between 0.1 and $1\,cm^2\,V^{-1}\,s^{-1}$ have been measured.[28–31]

Although the materials that form molecular crystals shown in Figure 1 exhibit very high charge carrier mobilities, they are not very attractive candidates for large-scale application because they have similar cost-disadvantages as inorganic semiconductors; they need to be prepared by vacuum evaporation. There has been some work on organic single-crystal transistors that can be processed from solution, but charge carrier mobilities as high as those in pentacene have not been reached for these crystals.[22] The growth of crystals from solution generally does not lead to homogeneous single-crystalline layers, leading to inferior charge transport properties compared to single crystal devices. For these reasons there is a considerable interest in the design of organic materials that can be processed from solution, while retaining high charge carrier mobilities.

Substituted conjugated polymers are organic semiconductors that can be processed from solution; *e.g.* by spin coating[32] or ink-jet printing.[33,34] Some examples are shown in Figure 2. For these materials the charge carrier mobilities that are measured in devices are generally several orders of magnitude lower than those for the single crystal materials discussed above. The low mobilities are mostly due to the structural disorder in these materials, which leads to energetic disorder and poor electronic coupling between neighbouring chains. The effect of structural organization on the charge transport properties is nicely illustrated by mobilities measured in transistors using poly-3-hexylthiophene (P3HT) as the active layer. The mobility of charges in P3HT was found to depend strongly on the positioning of the hexyl side chains on the backbone.

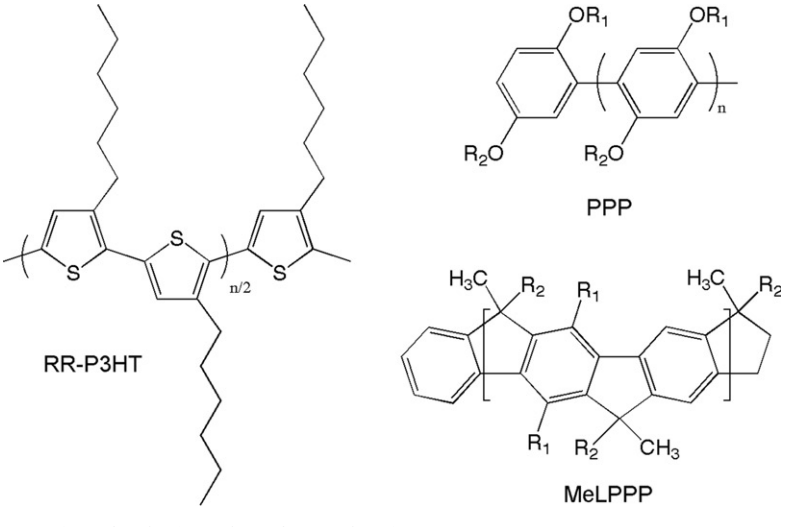

Figure 2. Examples of substituted conjugated polymers.

A regular substitution pattern leads to an ordered lamellar structure. The mobility in transistors based on highly ordered P3HT was found to be as high as[35] $0.1\,cm^2\,V^{-1}\,s^{-1}$, which is the highest value reported for polymer-based devices. A similar dependence of the charge carrier mobility on the supramolecular order induced by alkyl side chains has been reported for poly(phenylene-vinylene).[36]

Apart from the improved order on a supramolecular level, the intrachain organization is also known to have a pronounced effect on transport of charges. This was shown recently by microwave conductivity measurements of the intrachain mobility of charges along isolated ladder-type poly-*p*-phenylene (Me-LPPP) chains. Me-LPPP consists of linked phenyl units that are kept in a planar conformation by bridging carbon atoms (see Figure 2). For this polymer an intrachain mobility of $600\,cm^2\,V^{-1}\,s^{-1}$ was derived,[37] which is of the same order of magnitude as values found in inorganic semiconductors. The value of $600\,cm^2\,V^{-1}\,s^{-1}$ is $\sim$20 times higher than the largest value reported for molecular crystals[25] ($35\,cm^2\,V^{-1}\,s^{-1}$). This can be understood by considering the magnitude of the charge transfer integrals (also termed bandwidth integral or electronic coupling)[38] in these systems. The charge transfer integral for intramolecular charge transport along phenyl based polymer chains is of the order of 0.5 eV, whereas in organic molecular crystals it is close to 0.1 eV. The mobility increases with the magnitude of the charge transfer integral. Therefore the mobility along Me-LPPP chains can be expected to be higher than for organic molecular crystals. Even though the mobility values in molecular crystals are the highest found in organic materials, a significant increase of the mobility could be achieved by realization of a molecular arrangement for which the charge transfer integral is higher. In most organic crystals the molecules are either packed in a herring-bone type of structure (tetracene, pentacene, sexithiophene) or very displaced structure (rubrene) with little direct interaction between the π-systems of neighbouring molecules.[39,40] This leads to relatively small charge transfer integrals between neighbouring molecules. It is clear that there is considerable room for improvement of the charge transfer integrals by optimization of the structure on a supramolecular level, even for molecular crystals.

A natural strategy to control the ordering in a material on the molecular scale is to take advantage of molecular self-assembly.[41–44] In this approach, molecular building blocks self-organize into complex, relatively well-defined structures through intermolecular interactions such as aromatic π-stacking and hydrogen bonding. Widely studied self-organizing organic materials for opto-electronic applications are liquid-crystalline materials; see Figure 3 for some examples. Some of the molecules for which crystals are produced from the gas phase can be converted into liquid crystalline materials. Examples are quaterthiophene to which hexyl chains are attached to the outer thiophene rings[45,46] and phthalocyanine with alkyl chains attached.[47,48] The latter is an example of a whole class of materials called discotic liquid crystalline materials that have been studied extensively for opto-electronic applications.[49–56] Discotic molecules consist of a disc-like planar aromatic core with aliphatic side chains attached to it. These molecules are known to self-assemble into columnar structures forming stacks of the aromatic cores that are isolated from each other by the surrounding mantle of alkyl or alkoxy chains, (see Figure 4). The overlapping π-orbitals in the stack of aromatic cores provide one-dimensional pathways for charge transport. A wide variety of aromatic cores have been considered, ranging from relatively small triphenylenes to hexabenzocoronenes and even larger cores that resemble graphite layers.[52] Other discotic molecules are porphyrins and

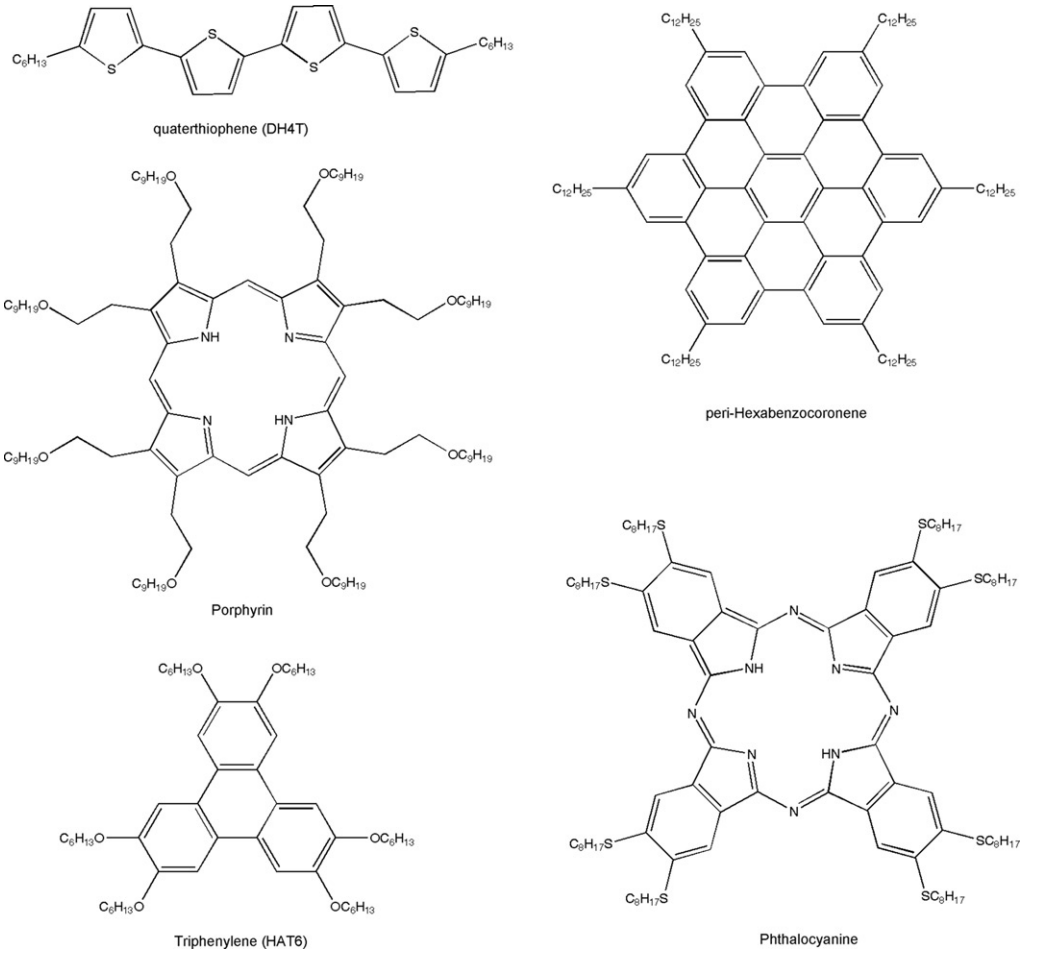

Figure 3. Examples of conjugated molecules that exhibit liquid crystalline phases.

phthalocyanines of which the unsubstituted molecule forms molecular crystals. As described in Section 4.1 mobilities of charge carriers in a variety of discotic liquid crystalline materials were obtained from AC conductivity,[50] time-of-flight (TOF)[53] and transistor measurements.[57,58] The highest mobilities reported for discotic materials are close to $1\,cm^2\,V^{-1}\,s^{-1}$ for derivatives of hexabenzocoronene.[59,60] An interesting property of discotic materials is the existence of a liquid crystalline phase. In this phase the aliphatic side are relatively free to move, while the columnar structure is maintained. In most cases the transition to this liquid crystalline phase leads to a lower charge carrier mobility than in the crystalline phase, most likely due to an enhanced degree of structural disorder. This shows that charge transport properties of these materials are very sensitive to subtle changes in the supramolecular order.

The way in which discotic materials self-assemble in solids is rather difficult to predict since aromatic interactions that favour π-stacking do not have a very specific

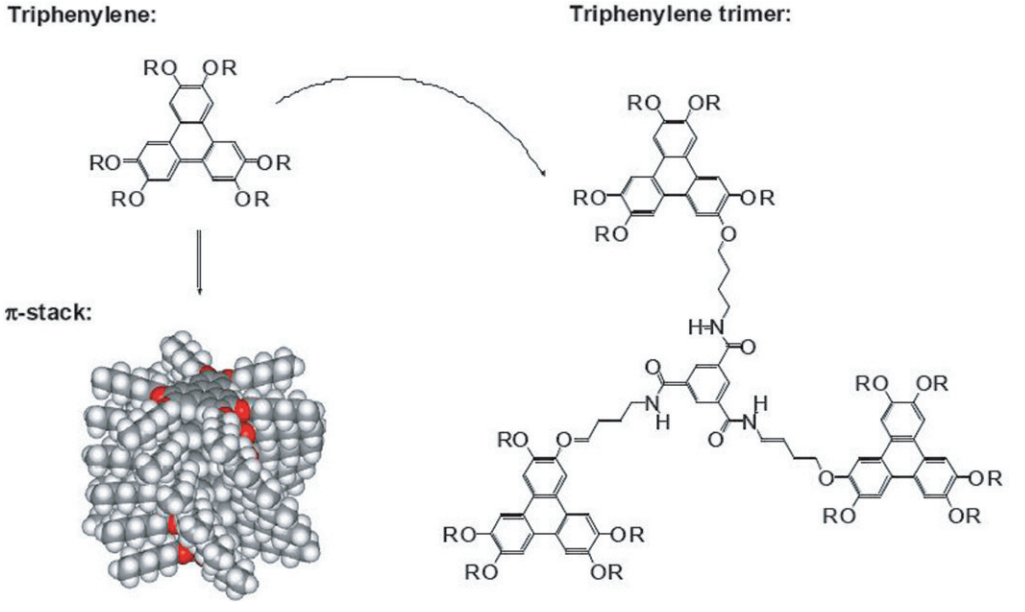

Figure 4. Three triphenylene (HAT6) connected to a central hydrogen-bonding unit. The hydrogen bonding leads to a structure that exhibits a higher charge carrier mobility compared to HAT6 without the hydrogen bonding units.

directionality. A high directionality of interactions can be achieved by using units that form hydrogen bonds. An example of this is shown in Figure 4. In this structure three discotic triphenylene molecules are connected to a trisamide unit.[61] These triphenylene trimers can form π-stacked structures in which hydrogen bonds are formed between the trisamides and the triphenylene units are stacked on top of each other with a very small twist angle between neighbouring discs. It was shown recently that this leads to a charge carrier mobility that is roughly five times higher than found for the material based on the individual triphenylene molecules.[61] Another example of the use of hydrogen bonding units to influence the supramolecular organization is shown in Figure 5. It has been shown that the orientation of oligothiophenes with respect to each other can be changed from a herring bone structure to a parallel displaced organization by attaching urea units that can form hydrogen bonds.[62]

Many of the self-assembly motifs used in the field of supramolecular chemistry find their inspiration in nature where molecular self-assembly is the basis of the large functional structures in living organisms. Examples of these self-assembled structures are the secondary and tertiary structure of proteins, the organization of chlorophylls in light-harvesting complexes, and the π-stacked structure of DNA that is held in place by hydrogen bonds between the nucleobases in the opposite strands. As discussed in Section 4.2 self-assembled stacks of hydrogen bonded dimers of oligo(phenylene-vinylene) molecules in solution can provide a pathway for charge transport. The mobility of charge carriers along stacks of two dimensional oligo(phenylene-vinylene) molecules is discussed in Section 4.3.

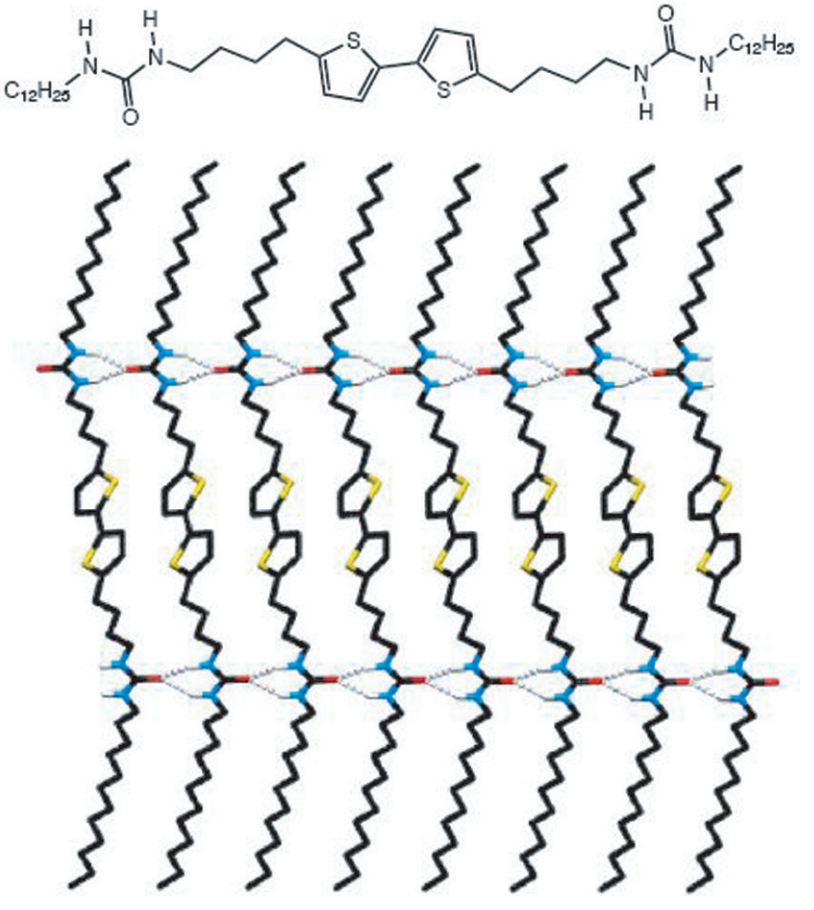

Figure 5. Bithiophene substituted with two urea units. Hydrogen bonding between the urea groups leads to highly ordered structures in the solid.

Charge transport along DNA has been studied extensively over the last two decades.[63–65] The possibility of electrical conductivity in DNA was put forward for the first time by Eley and Spivey in 1962,[66] briefly after Watson and Crick described the double helical structure.[67] Eley and Spivey noted that the stack of aromatic base pairs in the interior of the helix shows a striking resemblance to the stacking found in one-dimensional molecular crystals. There are also important differences between DNA and these materials. Natural DNA consists of a non-periodic stack of different nucleobases. This leads to energy variations along the stack that are much larger than for aromatic crystals and discotic materials, where all molecules are the same. Moreover, the structure of DNA in its natural aqueous environment is inherently flexible, and structural variations can be expected to influence the efficiency of charge transport to a large extent. The mechanism of charge migration through DNA attracts a great deal of interest because of relevance to oxidative strand cleavage, to the development of nanoelectronics, biosensor devices, and electrochemical sequencing techniques. Experimental and theoretical results

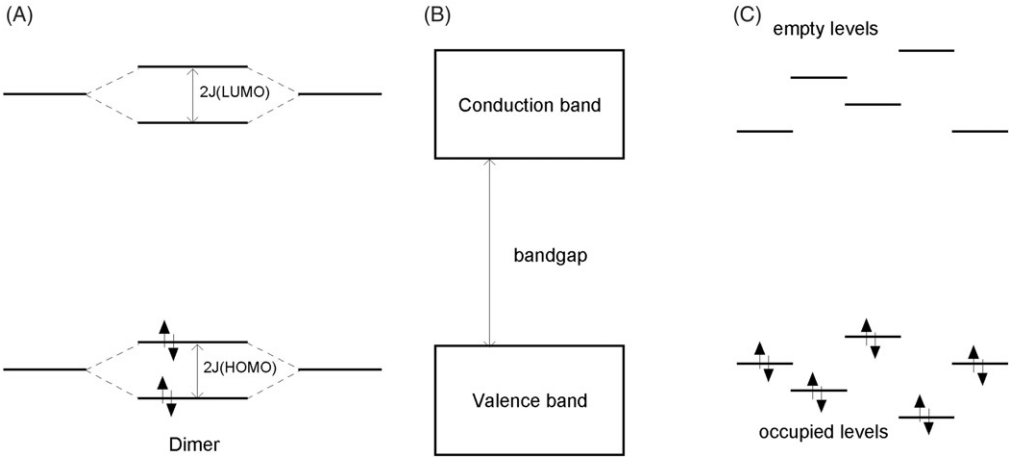

Figure 6. Schematic representation of the energy levels in a dimer of two conjugated molecules (A), bands in an ordered system (B), and discrete levels in a disordered molecular material (C). It is assumed that the spatial overlap integral, S, is zero so that the orbiatal splitting in a dimer is twice the charge transfer integral; *i.e.* $2J$.

obtained so far refer to the motion of positive charges (holes) rather than to the migration of excess electrons. For recent reviews on charge transport through DNA, see, *e.g.*[64,65,68]

The organic materials discussed above can be considered as wide band gap semiconductors with a typical band gap of a few eV. The electronic structure of organic semiconductors is illustrated in Figure 6. When two molecules come close together their orbitals start to interact. When only the highest occupied molecular orbitals (HOMOs) are considered this leads to the formation of two new energy levels with an energy splitting that is close to twice the charge transfer integral between the two HOMOs. For the lowest unoccupied molecular orbitals (LUMOs) an analogous splitting occurs. When an infinite number of molecules are brought together in a regular structure (*i.e.* a molecular crystal), the HOMOs (LUMOs) on the different molecules interact to form continuous bands of energy levels. At zero temperature the band formed by the HOMOs, the valence band, is completely filled with electrons, while the conduction band that is formed from the LUMOs is empty. In organic materials the gap between the valence and conduction band is much larger than the thermal energy at room temperature. Therefore, electrons are hardly excited thermally from the valence to the conduction band and organic materials behave as insulators. Organic materials can become conducting by adding dopants, by injection of charges from electrodes or by photoexcitation of an electron from the valence to the conduction band. The formation of valence and conduction bands that are delocalized through the whole material requires a periodic structure, which may to a large extent be realized in molecular crystals. However, in more disordered materials such as discotics and conjugated polymers electronic bands are usually not formed and a distribution of discrete energy levels localized on one or a few molecular units exists (see Figure 6). The two models sketched here are extreme cases and the actual nature of electronic states depends strongly on the supramolecular order in the material.

As discussed in the material morphology at the molecular level also determines the parameters important for charge transport, including the charge transfer integral, site energy disorder and reorganization energy.

In the Section 2 different theoretical frameworks for charge transport are discussed. In Section 3 methods to calculate parameters of relevance to charge transport are described. In Section 4 the factors governing the mobility of charge carriers in some examples of self-organizing materials are discussed on basis of concepts and models introduced in Section 2.

2. Theory of charge carrier mobility

2.1. *Definition of charge carrier mobility*

The current density due to charge carriers with number density n moving in an electric field is given by

$$j(t) = e\, n\, v_d(t). \tag{2}$$

In Equation (2) e is the elementary charge and $v_d(t)$ is the mean drift velocity of charge carriers at time t, which is superimposed on their stochastic diffusive motion. The time-dependence in Equation (2) accounts for the possible oscillating behaviour of the electric field. Under common circumstances the oscillation frequency is sufficiently low, so that the wavelength of the associated electromagnetic field largely exceeds the spatial extent of the charge carriers. In this so-called local limit the dipole approximation can be made, which implies setting the wave vector of the electromagnetic field equal to zero,[69,70] so that the AC electric field can be written as

$$E(t) = E_0 \cos(\omega t) \tag{3}$$

with E_0 the electric field strength and ω the radial frequency. For sufficiently small electric field strength the limit of linear response is valid and the drift velocity of the charge carriers is given by

$$v_d(t) = \mu'(\omega) E_0 \cos(\omega t) + \mu''(\omega) E_0 \sin(\omega t). \tag{4}$$

The first term on the right-hand side of Equation (4) is the velocity component of the charge carriers in-phase with the oscillating electric field. The in-phase velocity is proportional to the real part, $\mu'(\omega)$, of the complex mobility. The second term on the right-hand side of Equation (4) is the out-of-phase velocity component, which is proportional to the imaginary part, $\mu''(\omega)$, of the mobility. Note that the out-of-phase component of the velocity vanishes at zero frequency (DC limit: $\omega = 0$). At non-zero frequency ($\omega \neq 0$) the velocity component in-phase with the electric field causes the charge carriers to absorb power from the AC field, leading to attenuation of the field strength. The out-of-phase component of the charge carrier drift velocity corresponds to a polarizability of the medium and causes a reduction of the propagation speed of the electromagnetic waves associated with the AC field. This leads to a phase shift of the AC field after having traversed the conducting medium. The complex mobility is related to the complex conductivity according to

$$\sigma = en\mu. \tag{5}$$

The mobility of charge carriers in solids with a periodic structure is often described in terms of the semiclassical Boltzmann transport equation.[2,69–71] More rigorous approaches start from a quantum mechanical transport theory.[71–74] The linear response formalism due to Kubo provides a general starting point for a semiclassical or a fully quantum mechanical description of the mobility.[72,75–77] For charge carriers at thermal equilibrium moving in an electric field along the x-direction the complex mobility is according to Kubo's formula given by

$$\mu(\omega) = \frac{e}{k_B T}\int_0^\infty \langle v_x(t)v_x(0)\rangle e^{-i\omega t}\,\mathrm{d}t = -\frac{e\omega^2}{2k_B T}\int_0^\infty \langle (x(t)-x(0))^2\rangle e^{-i\omega t}\,\mathrm{d}t \tag{6}$$

with k_B boltzmann's constant and T the temperature. An implicit convergence factor $e^{-\varepsilon t}$ ($\lim \varepsilon \to 0$) is understood in the integral.[75,76,78] In Equation (6) v_x is the component of the thermal velocity of a charge carrier along the x-direction; *i.e.* the velocity in absence of an electric field. On application of an electric field the drift velocity in Equation (4) is superimposed on the thermal velocity v_x in Equation (6). The mean square displacement along the x-direction in Equation (6) corresponds to the thermal diffusive motion of the charges in absence of an electric field. The brackets, $\langle\,\rangle$, imply averaging over a large number of charge carriers at thermal equilibrium. Note, that for isotropic systems the velocity autocorrelation function in Equation (6) can be written as $\langle v_x(t)v_x(0)\rangle = \langle v(t)v(0)\rangle/d$ with v the total velocity and $d=1$, 2, 3 the dimensionality of the system. Similarly one can write $\langle (x(t)-x(0))\rangle^2 = \langle |\mathbf{r}(t)-\mathbf{r}(0)|^2\rangle/d$ with $\mathbf{r}$ the total displacement vector.

Calculation of the charge carrier mobility on basis of Equation (6) involves evaluation of the average velocity autocorrelation function, or averaging the square displacement for all charge carriers contributing to the conductivity. This averaging involves taking the contribution of all (quantum) states of the charge carriers, weighted with their occupation probability. The charge carrier states can be obtained from the Hamiltonian of the system, which is given by[79–81]

$$H = H_e + H_{ph} + H_{e-ph}. \tag{7}$$

In Equation (7) H_e is the pure electronic Hamiltonian and H_{ph} is the bare phonon Hamiltonian. The Hamiltonian H_{e-ph} describes interactions between electrons and phonons, associated with dynamic structural fluctuations in the material. Such fluctuations may correspond to vibrations of the nuclei within a molecular unit or to motions of entire molecular units.

For molecular materials the tight-binding method is an appropriate starting point to describe electron states as a superposition of states $|\varphi_s^\kappa\rangle$ that are localized on the molecular units s.[2,71,79,80] The total wavefunction of a charge carrier coupled to phonons can then be written in the general form[82]

$$|\Psi_\kappa\rangle = \sum_s C_s^\kappa \left|\varphi_s^\kappa\right\rangle\left|\chi_s^\kappa\right\rangle \equiv \sum_s C_s^\kappa |s,\kappa\rangle \tag{8}$$

with C_s^κ the expansion coefficient of the state $|s,\kappa\rangle$, which describes a charge localized at molecular unit s, and with the index κ labelling the dynamic (phonons) and static

structural fluctuations. The phonons are described by the states, $|\chi_s^\kappa\rangle$, associated with a charge at site s. Calculation of the mobility with Equation (6) involves averaging over the density distribution of the charge $\rho = \sum_\kappa P_\kappa |\Psi_\kappa\rangle\langle\Psi_\kappa|$, with P_κ the population of the state with index κ.

In the case of normal Gaussian diffusion the mean square displacement of a charge eventually increases linearly with time, according to

$$\left\langle \left|\mathbf{r}(t) - \mathbf{r}(0)\right|^2 \right\rangle = 2\,d\,Dt \tag{9}$$

with D the diffusion constant. Substitution of Equation (9) into Equation (6) gives the Einstein relation for the mobility

$$\mu = \frac{e}{k_B T} D. \tag{10}$$

The mobility in Equation (10) is frequency independent and the imaginary component is zero. It should be noted that structural defects in a material can lead to barriers for charge transport. In that case charge transport is dispersive and the mean square displacement increases sublinearly with time, so that the mobility is no longer given by Equation (10). Barriers cause the mobility to be frequency dependent and to consist of non-zero real and imaginary components. Measurements of the frequency dependent real and imaginary components of the AC mobility can provide information about the effects of barriers to charge transport and on the ultimate mobility that can be achieved in absence of barriers.[37,83–88] Time-resolved microwave[83] and terahertz[89] conductivity techniques are very suitable to determine the frequency dependent complex mobility.

For one-dimensional rod-shaped systems, such as columns of π-stacked molecules or linear polymer chains, the measured mobility of charge carriers depends on the orientation of the rods with respect to the direction of the electric field. For rods that are aligned parallel to the field direction the mobility, $\mu_{||}$, of charges moving along the rod is given by Equation (6), with v_x the velocity along the rod. In the absence of charge transport between different rods the measured mobility is zero for a perpendicular arrangement of the rods with respect to the field direction. For rods at polar angle Θ with respect to the field, the component of the charge velocity along the field direction decreases by a factor $\cos(\Theta)$ and according to Equation (6). The measured mobility then reduces by a factor $\cos^2(\Theta)$. Hence, for an isotropic distribution of rods the average measured mobility is equal to $\overline{\mu} = (\int_0^\pi \cos^2(\Theta) d\cos(\Theta) / \int_0^\pi d\cos(\Theta))\mu_{||} = (1/3)\mu_{||}$.

2.2. *Band model for delocalized charges in ordered materials*

In case charge carriers only interact weakly with the nuclear lattice a zero-order adiabatic description invoking the Born–Oppenheimer approximation is appropriate. For a structurally ordered material with a periodic structure the electronic states take the form of Bloch functions.[71,90] In the case of molecular materials the tight-binding model provides a proper description of the electronic states, which can be expressed as[2,71,80]

$$\left|\Psi_k(\mathbf{r})\right\rangle = f_N \sum_s \exp(i\mathbf{k}\cdot\mathbf{r}_s)\left|\varphi(\mathbf{r}-\mathbf{r}_s)\right\rangle. \tag{11}$$

In Equation (11) $\mathbf{k}$ is the wave vector of the charge carrier and $|\varphi(\mathbf{r}-\mathbf{r}_s)\rangle \equiv |\varphi_s\rangle$ is an electronic state localized at the molecular unit with position vector $\mathbf{r}_s$ and f_N is the normalization constant. Note, that the states $|\varphi_s\rangle$ may depend on the wave vector $\mathbf{k}$.[91] However, for excess electrons with energies near the bottom of the conduction band or excess positive charges (holes) near the top of the valence band, this $\mathbf{k}$ dependence is usually negligible. In that case the lowest unoccupied molecular orbitals (LUMOs) or the highest occupied molecular orbitals (HOMOs) can provide an appropriate representation of the states $|\varphi_s\rangle$ for excess electrons or holes, respectively.

In the adiabatic (or Born–Oppenheimer) approximation the electron–phonon interaction is neglected and the Hamiltonian of a charge carrier can be written as

$$H_{el} = \sum_s \varepsilon_s a_s^+ a_s + \sum_{s,\, s' \neq s} J_{s,s'} a_s^+ a_{s'} \tag{12}$$

with a_s^+ and a_s the creation and annihilation operators of a charge at molecular unit s. The site energy is the energy of a charge carrier when it is localized on a molecular unit and is given by the diagonal Hamiltonian matrix element $\varepsilon_s = \langle\varphi_s|H_{el}|\varphi_s\rangle \equiv \varepsilon$, with the last equality being valid since all sites are identical for a periodic structure. The off-diagonal matrix elements of the Hamiltonian $J_{s,s'} = \langle\varphi_s|H_{el}|\varphi_{s'}\rangle$ are the so-called charge transfer integrals (also referred to as electronic coupling, bandwidth or hopping integral). The charge transfer integrals determine the rate of charge transfer between the molecular units and in turn the mobility of charge carriers. Using Equations (11) and (12) implies that Coulomb interactions between different excess charges are neglected, which is valid for low charge carrier density. However, interactions of an excess electron (or hole) in the conduction (or valence) band with other bound electrons in the system is included via the values of the site energies and charge transfer integrals, together with the Coulomb interactions with the nuclei. For reasons of clarity the band energies are now considered for a one-dimensional structure of molecular units with mutual spacing a. Due to the localized nature of the molecular states it is a good approximation to only take charge transfer integrals between nearest neighbours into account; *i.e.* $s' = s \pm 1$ in Equation (12). The spatial overlap, $S_{s,s+1} = \langle\varphi_s|\varphi_{s+1}\rangle$, between electronic states on adjacent molecular units can be substantial and must therefore be taken into account,[81,82,92,93] in contrast to common use in the literature. For ordered periodic systems as considered in this section all site energies, charge transfer integrals and spatial overlap integrals are identical and the subscripts indicating the site indices can be omitted. The band energies obtained from Equations (11) and (12) are then given by

$$E_k = \frac{\langle\Psi_k|H_{el}|\Psi_k\rangle}{\langle\Psi_k \mid \Psi_k\rangle} = \frac{\varepsilon + 2J'\cos(ka) - 2J''\sin(ka)}{1 + 2S'\cos(ka) - 2S''\sin(ka)} \tag{13}$$

for the general case in which the nearest-neighbour charge transfer integral $J = J' + iJ''$ ($i^2 = -1$) and the spatial overlap integral $S = S' + iS''$can be complex numbers.[93] Equation (13) was derived for the one-dimensional case. In two- or three-dimensional systems additional terms containing charge transfer and overlap integrals for the other dimensions appear in the numerator and denominator, analogous to those in Equation (13). Usually the spatial overlap is sufficiently small so that $1/(1+S) \approx 1 - S$.

Using this approximation and neglecting terms containing the product of S and J, Equation (13) can be written as

$$E_k = \varepsilon + 2(J' - S\varepsilon)\cos(ka) - 2(J'' - S''\varepsilon)\sin(ka)$$
$$\equiv \varepsilon + 2J'_{eff}\cos(ka) - 2J''_{eff}\sin(ka) \tag{14}$$

with the effective (or generalized) charge transfer integral defined as[38,82]

$$\left(J_{eff}\right)_{s,s'} = J_{s,s'} - S_{s,s'}\left(\frac{\varepsilon_s + \varepsilon_{s'}}{2}\right). \tag{15}$$

The expressions in Equation (14) shows that the effect of the spatial overlap between localized electronic states on adjacent molecular units has been accounted for by using effective charge transfer integrals. When effective charge transfer integrals are used, the spatial overlap no longer needs to be taken into account explicitly.

The results for the band energies and the Bloch states considered above do not include effects of scattering of charge carriers due to interactions with phonons or static lattice imperfections. In a band-like description, as considered in this section, scattering events are treated as small perturbations, leading to transitions between Bloch states with different **k** vectors, or equivalently, with different velocity. Scattering causes the velocity autocorrelation function in the Kubo formula for the mobility [Equation (6)] to decay during time. In case scattering does not depend on the magnitude and the direction of the velocity (isotropic scattering), or when scattering is elastic, the relaxation time approximation is applicable and the velocity autocorrelation function decays exponentially according to[69,94,95]

$$\langle v_x(t)v_x\rangle = \langle v_x^2\rangle \exp\left(\frac{-t}{\tau}\right). \tag{16}$$

Insertion of Equation (16) into the Kubo formula Equation (6) yields for the mobility

$$\mu = \frac{e}{k_B T}\langle v_x^2\rangle \frac{\tau}{1 + i\omega\tau} \tag{17}$$

which for a constant electric field ($\omega = 0$) reduces to the DC mobility

$$\mu_{DC} = \frac{e}{k_B T}\langle v_x^2\rangle \tau. \tag{18}$$

2.2.1. *Wide band materials*

In case the width of the energy band in Equation (14), or equivalently the magnitude of the effective charge transfer integral, is much larger than thermal energy, $k_B T$, excess electrons will occupy states near the bottom of the conduction band, while holes will be close to the top of the valence band. Near these band extrema (which occur at wave vector k_0 for which

$\tan(k_0 a) = -J''_{eff}/J'_{eff}$) the energies in Equation (14) can be approximated by a second order Taylor expansion with respect to k, giving

$$E_k = \frac{\hbar^2(k-k_0)^2}{2m^*} = \frac{1}{2}m^* v^2 \tag{19}$$

with the effective mass of the charge carrier

$$m^* = \hbar^2 \left(\left(\frac{\mathrm{d}^2 E}{\mathrm{d}k^2} \right)_{k=k_0} \right)^{-1} = \frac{\hbar^2}{2a^2 |J_{eff}|} \tag{20}$$

and the velocity $v = \hbar^{-1}(\mathrm{d}E/\mathrm{d}k) = \hbar(k-k_0)/m^*$.

For isotropic two- or three-dimensional systems the results are identical to those in Equations (19) and (20) with k the total magnitude of the wave vector of the charge carrier. For the molecular materials considered the effective mass of excess electrons and holes is usually comparable, so that the Fermi level is near the middle of the band gap, which largely exceeds thermal energy, $k_B T$.[2] Hence, the distribution of charge carriers over different energies can be described using Boltzmann statistics, yielding

$$\langle v_x^2 \rangle = \frac{k_B T}{m^*}. \tag{21}$$

Insertion of Equation (21) into Equations (17) and (18) yields for the mobility

$$\mu = \frac{e}{m^*} \frac{\tau}{1+\omega^2\tau^2} - i \frac{e}{m^*} \frac{\omega\tau^2}{1+\omega^2\tau^2} \tag{22}$$

and the DC mobility

$$\mu_{DC} = \frac{e}{m^*}\tau = \frac{2ea^2|J_{eff}|}{\hbar^2}\tau. \tag{23}$$

The result in Equation (22) is of the Drude form[69,94] with the free electron mass replaced by the effective mass of the charges. In Equation (16) the scattering time τ was assumed to be independent of the magnitude of the velocity of the charge carrier. If the dependence of the scattering time on charge velocity is taken into account the DC mobility can be calculated using the energy weighted scattering time $\bar{\tau} = \langle E\tau(E)\rangle / \langle E \rangle = \int \tau(E) E^{d/2} f(E) \mathrm{d}E / \int E^{d/2} f(E) \mathrm{d}E$ with $f(E)$ the Fermi–Dirac distribution function and $d = 1, 2, 3$ the dimensionality of the system.[2,95]

Note, that the Drude type expression for the mobility in Equations (22) and (23) is only valid in case the energy of the charge carriers depends quadratically on their velocity according to Equation (19) and scattering causes the velocity autocorrelation function to decay exponentially as in Equation (16). These conditions are not fulfilled when charge carriers undergo strong interactions with phonons or scattering on structural imperfections. This restricts the applicability of the Drude type mobility to structurally ordered systems in which charge carriers only undergo weak scattering. Weak scattering means that the width, $W = 4|J_{eff}|$, of the energy band in Equation (14) largely exceeds the energy uncertainty, ΔE, due to scattering induced mixing of Bloch states with different wave vector $\mathbf{k}$;[2,80] *i.e.* $W \gg \Delta E > \hbar/\tau$, or $\tau \gg \hbar/W$. For the band-like model discussed above

combination of the latter condition with Equations (20) and (23) yields the following lower limit to the mobility

$$\mu > \frac{ea^2}{2\hbar}. \tag{24}$$

In π-stacked molecular materials and conjugated polymers the typical distance, a, between molecular units is 0.35 nm. According to Equation (24) a mobility exceeding $1\,cm^2\,V^{-1}\,s^{-1}$ is a necessary (but not sufficient) condition for the band model to be valid. With the exception of oligoacene molecular crystals typical charge carrier mobilities in organic materials are lower than $1\,cm^2\,V^{-1}\,s^{-1}$ and the band model is not valid. However, the band model may be appropriate to describe the high intrachain charge carrier mobility of $600\,cm^2\,V^{-1}\,s^{-1}$, measured for structurally ordered planar ladder-type Me-LPPP chains in dilute solution.[37] High intrachain charge carrier mobilities of a few tens of $cm^2\,V^{-1}\,s^{-1}$ have also been found for MEH-PPV[82,85] and a derivative of polyfluorene in dilute solution.[96] However, the non-periodic structure due to torsional disorder and chain coiling for MEH-PPV and polyfluorene in solution, do not allow to apply the band model to these materials. In solid Me-LPPP, interchain interactions lead to a non-periodic structure and consequently the band model cannot be applied, despite the high intrachain charge carrier mobility of[84] $30\,cm^2\,V^{-1}\,s^{-1}$. For the non-periodic polymer chains the models described in Section 2.3 have been found appropriate.[82,85,96]

The electron–phonon scattering time in Equations (22) and (23) decreases with temperature, which leads to a reduction of the mobility. In addition, electron–phonon interactions can lead to a narrowing of the bandwidth, which is due to a renormalization of the charge transfer integral with a factor that is determined by the magnitude of the electron–phonon coupling.[97–100] This effect enhances the effective mass of the charge carrier and leads to a thermally deactivated mobility for temperatures below the Debye temperature. At higher temperatures the enhanced structural fluctuations can lead to a transition from band like charge transport to thermally activated hopping. Recent theoretical studies on effects of temperature on bandwidths and in turn the mobility of charge carriers in oligoacene crystals have been reported in references.[101–103]

The mobility decreases with the frequency ω of the electric field. At low frequencies the charge carriers undergo many scattering events during an oscillation period of the electric field and their velocity is in-phase with the field. As a result the imaginary component of the mobility is small. At higher frequencies the ballistic regime is reached in which the velocity of the charges becomes out-of-phase with the electric field. In this regime the imaginary component of the mobility dominates over the real component. The frequency dependence of the Drude type mobility discussed above is a result of the relaxation time approximation in Equation (16), which implies that the velocity of charge carriers randomizes after a scattering event. Extensions of the Drude model to cases in which the original velocity of charge carriers is at least in part retained after a scattering event are discussed in[104] and references therein.

2.2.2. *Narrow band materials*

In case the bandwidth is small compared to thermal energy, k_BT, charge carriers will be close to uniformly distributed over all Bloch states in the energy band. Hence, the mean

square velocity in Equations (17) and (18) can now be evaluated to a good approximation by averaging over all wave vectors k in the first Brillouin zone. Using $v_x = \hbar^{-1}\mathrm{d}E/\mathrm{d}k$ together with Equation (14) and averaging over k yields for the mobility

$$\mu = \frac{e}{k_B T}\frac{2a^2}{\hbar^2}\left|J_{eff}\right|^2\tau. \tag{25}$$

As discussed in Section 2.2.1 the band model is valid in the limit of weak scattering, so that $\tau > \hbar(4|J_{eff}|)$, which implies that

$$\mu > \frac{ea^2}{2k_B T\hbar}\left|J_{eff}\right|. \tag{26}$$

For $|J_{eff}| = k_B T$ (*i.e.* the narrow band limit for which thermal energy is comparable with the band width) and $a = 0.35\,\mathrm{nm}$ the condition in Equation (26) yields that the band model may be appropriate only in case the mobility is higher than $1\,\mathrm{cm}^2\,\mathrm{V}^{-1}\,\mathrm{s}^{-1}$; which is the same value as found for wide band materials discussed in Section 2.2.1.

2.3. *Tight-binding models for delocalized charges in weakly disordered materials*

Molecular organic materials such as conjugated polymers and self-assembling π-stacked systems usually exhibit significant structural disorder. Disorder can be due to static and dynamic fluctuations of the molecular geometry and the mutual arrangement of molecules. In addition, chemical defects and impurities will affect charge motion. In the presence of such disorder, scattering of charge carriers on structural or chemical defects can no longer be treated as a small perturbation and the band-like description of Section 2.2 is no longer appropriate. A description of charge carrier motion now proceeds from the complete Hamiltonian in Equation (7), which takes into account interactions between the electron and dynamic structural fluctuations (phonons) and static defects.

To calculate the mobility of charge carriers the mean square displacement in Equation (6) is evaluated by using the Heisenberg representation for the time-dependent position operator; *i.e.* $x(t) = \mathrm{e}^{iHt/\hbar}x\,\mathrm{e}^{-iHt/\hbar}$.[105] Using Equation (8) for the wavefunction of the system, it is found that[82]

$$\begin{aligned}\left\langle (x(t)-x)^2\right\rangle &= \mathrm{Tr}\left[(x(t)-x)^2\rho\right] = \sum_{\kappa} P_\kappa \langle\Psi_\kappa|(x(t)-x)^2|\Psi_\kappa\rangle \\ &= \sum_{\kappa,\kappa''}\sum_{s,s',s''} P_\kappa C_s^\kappa \left(C_{s'}^\kappa\right)^* a^2\left[(s'')^2 - s''(s+s')\right]\left\langle s',\kappa\right|\mathrm{e}^{iHt/\hbar}\left|s'',\kappa''\right\rangle\left\langle s'',\kappa''\right|\mathrm{e}^{-iHt/\hbar}\left|s,\kappa\right\rangle \\ &\quad + \sum_{\kappa}\sum_{s} P_\kappa C_s^\kappa \left(C_s^\kappa\right)^* a^2 s^2.\end{aligned} \tag{27}$$

The factor $\langle s'',\kappa''|\mathrm{e}^{-iHt/\hbar}|s,\kappa\rangle$ in Equation (27) is the coefficient of the state $|s'',\kappa''\rangle$ at time t, of a charge that was initially ($t=0$) in the state $|s,\kappa\rangle$, localized at molecular unit s. Analogously, the factor $\langle s',\kappa|\mathrm{e}^{iHt/\hbar}|s'',\kappa''\rangle$ is the complex conjugate of the coefficient of $|s'',\kappa''\rangle$ for a charge initially localized at s' in the state $|s',\kappa\rangle$. Hence, these coefficients correspond to charge migration from different initial sites to a common final site. The summation over κ in Equation (27) leads to averaging of the products of the coefficients for these different paths over realizations of molecular systems with distinct static and

dynamic structural fluctuations. The different structural conformations and fluctuations will cause the phase of these expansion coefficients to vary from one system to another. As a consequence averaging over κ will cause the contribution of terms for which $s \neq s'$ in Equation (27) to vanish on a timescale referred to as the dephasing (or decoherence) time. This dephasing time is determined by the amplitude and frequency of the fluctuations. The vanishing of the average of the cross-product terms with $s \neq s'$ in Equation (27) is analogous to the relaxation of the off-diagonal elements of the density matrix (in terms of localized states) of a particle moving under the influence of stochastic fluctuations due to interactions with a heat bath.[79,106–108] In summary, due to the effects of structural fluctuations, the terms in Equation (27) for which $s \neq s'$ can often, to a good approximation, be neglected. In that case Equation (27) reduces to

$$\left\langle (x(t)-x)^2 \right\rangle = \sum_{\kappa,\kappa''} \sum_{s,s''} P_\kappa \left| C_s^\kappa \right|^2 a^2 (s''-s)^2 \left| \left\langle s'', \kappa'' \right| \mathrm{e}^{-iHt/\hbar} |s, \kappa\rangle \right|^2. \tag{28}$$

Equation (28) describes the mean square displacement of charges that are initially localized at site s, which migrate during a time interval t to other sites s'' with a probability equal to

$$p_{s'',s} = \left| \left\langle s'', \kappa'' \right| \mathrm{e}^{-iHt/\hbar} |s, \kappa\rangle \right|^2. \tag{29}$$

Evaluation of the mean square displacement in Equation (28) with the full Hamiltonian in Equation (7) with a quantum mechanical description of the phonons is impractical. The nuclear motions affecting charge transport are often sufficiently slow so that they can, to a good approximation, be treated classically, *e.g.* by molecular dynamics simulations. Dynamic fluctuations can then be taken into account via a time-dependence of the site energies and the charge transfer integrals.[79,109–119] Static structural fluctuations and defects lead to a variation of the site energies and charge transfer integrals from one molecular unit to another. In this case the Hamiltonian of the charge can be written as

$$H^k(t) = \sum_s \varepsilon_s^\kappa(t) a_s^+ a_s + \sum_s \sum_{s'=s\pm1} J_{s,s'}^\kappa(t) a_s^+ a_{s'}. \tag{30}$$

The time-propagation of the nuclear coordinates is described by the classical equations of motion with a potential that is in part determined by the distribution of the charge in the system; *i.e.* by the wavefunction $|\Psi_\kappa\rangle$ in Equation (8). The mean square displacement in Equation (28) is obtained by propagation of wavefunctions, which are initially localized at a single site s; *i.e.*

$$\left| \psi_\kappa(t; s) \right\rangle = \sum_{s''} c_{s''}^\kappa(t; s) \left| \varphi_{s''}^\kappa \right\rangle \tag{31}$$

with the initial condition $c_{s''}^\kappa(t=0; s) = 1$ for $s'' = s$ and zero for all other sites. Note that the wavefunctions defined in Equation (31) are distinct from the wavefunctions $|\Psi_\kappa\rangle$ in Equation (8), which are stationary states describing the charged molecular wires. The time-dependent coefficients $c_{s''}^\kappa(t; s) = \langle \varphi_{s''}^\kappa | e^{-iH_q^\kappa(t)t/\hbar} | \varphi_s^\kappa \rangle$ can be obtained numerically by integration of the first-order differential equations that follow from the time-dependent Schrödinger equation. The time-dependence of the effective Hamiltonian in Equation (30) can be taken into account by using the time-dependent self-consistent field (TDSCF) method.[82,120] As follows from Equations (28) and (31), the mean square

displacement can now be obtained from the time-dependent expansion coefficients $c^{\kappa}_{s''}(t; s)$ according to

$$\left\langle (x(t) - x)^2 \right\rangle = \left\langle \sum_{s'', s} f(s) a^2 (s'' - s)^2 \left| c_{s''}(t; s) \right|^2 \right\rangle. \tag{32}$$

The brackets at the right-hand side indicate averaging over different realizations of the structural fluctuations (denoted by the index κ above) and $f(s)$ denotes the equilibrium charge density at site s. Hybrid numerical quantum-classical methodologies as outlined above have been used to describe charge transport in conjugated polymers,[82,85,96,112–116,121,122] organic molecular crystals[119] and DNA[123–127] with inclusion of static and/or dynamic structural fluctuations.

For special cases analytical results have been provided for the mean square displacement of excitons or charges moving in a one-dimensional system with fluctuating site energies and charge transfer integrals. The charge carrier is described in terms of the density matrix, which propagates during time according to the stochastic Liouville equation

$$\frac{\partial \rho(t)}{\partial t} = -\frac{i}{\hbar}[H_{el}, \rho(t)] - R\rho(t), \tag{33}$$

with H_{el} the pure electronic Hamiltonian in Equation (7) and R the Redfield relaxation operator, which takes into account the average effects of structural fluctuations on the motion of the charge carrier.[79,108,128] In the so-called site representation the matrix elements of the density operator are given by $\hat{\rho}_{ss'} = \langle \varphi_s | \rho | \varphi_{s'} \rangle = \langle \varphi_s | \psi \rangle \langle \psi | \varphi_{s'} \rangle$ with $|\psi\rangle$ the initial state of the charge carrier and $|\varphi_s\rangle$ a state localized at molecular unit s. The Redfield operator corresponds with a tetradic relaxation matrix often referred to as the Redfield relaxation tensor. The first term in Equation (33) describes coherent charge carrier motion in absence of fluctuations. The second term containing the Redfield operator accounts for incoherent transitions of the charge carrier between different molecular units (population transfer) and decay of the off-diagonal elements of the density matrix (dephasing or decoherence). Dephasing causes charge carrier motion to become diffusive.

An analytical expression for the mean square displacement has been provided for the case of white-noise-like uncorrelated fluctuations in the site energies, $\delta\varepsilon_s(t)$, and nearest-neighbour charge transfer integrals, $\delta J_{s,s'}(t)$, in Equation (30), so that $\varepsilon_s(t) = \varepsilon + \delta\varepsilon_s(t)$ and $J_{s,s'}(t) = (J + \delta J_{s,s'}(t))\delta_{s,s'\pm 1}$, with $\delta_{s,s'\pm 1}$ the Kronecker delta.[106,129] The fluctuations have zero mean value and are real. The second moments of the fluctuations have the form

$$\left\langle \delta\varepsilon_s(t)\delta\varepsilon_{s'}(t') \right\rangle = 2\gamma_0 \hbar \delta(t - t')\delta_{s,s'} \tag{34}$$

$$\left\langle \delta J_s(t)\delta J_{s'}(t') \right\rangle = 2\gamma_1 \hbar \delta(t - t')\delta_{s,s'}, \tag{35}$$

with $\delta(t - t')$ the Dirac δ-function. Equation (34) describes dynamic diagonal disorder, which leads to non-zero off-diagonal matrix elements of $R\rho$ in Equation (33) only; *i.e.* $(R\rho)_{s,s'} = -2(\gamma_0/\hbar)\rho_{s,s'}(1 - \delta_{s,s'})$. Equation (35) describes off-diagonal dynamic disorder and gives rise to both non-zero diagonal and off-diagonal matrix elements of $R\rho$. For dynamic disorder as defined by Equations (34) and (35) an analytical expression for the

mean square displacement has been provided.[106] Substitution of this result into Equation (6) yields for the frequency dependent mobility

$$\mu = \frac{ea^2}{k_B T}\left[\frac{2\gamma_1}{\hbar} + \frac{2J^2}{\hbar^2}\left\{\frac{\tau}{1+\omega^2\tau^2} - i\frac{\omega\tau^2}{1+\omega^2\tau^2}\right\}\right] \tag{36}$$

with the DC mobility for $\omega = 0$ given by

$$\mu_{DC} = \frac{ea^2}{k_B T}\left[\frac{2\gamma_1}{\hbar} + \frac{J^2}{\hbar(\gamma_0 + 3\gamma_1)}\right] \tag{37}$$

and $\tau = \hbar/(2(\gamma_0 + 3\gamma_1))$. Note that effects of non-zero spatial overlap can be taken into account by using the effective charge transfer integral defined in Equation (15) rather than J in Equations (36) and (37). The first term between square brackets in Equations (36) and (37) is due to fluctuations in the charge transfer integrals and is referred to as the incoherent part. Even in case of vanishing J the mobility is non-zero, due to this incoherent part. The second term between square brackets in Equations (36) and (37) is the coherent part, which describes band motion that is hindered by fluctuations in the site energies and charge transfer integrals. The coherent part vanishes as $J \to 0$.

The frequency dependent factor between curly brackets in Equation (36) has the Drude form (*cf.* Equation (22)). In the absence of fluctuations in the charge transfer integrals ($\gamma_1 = 0$) the mobility vanishes at high frequency. However, for non-zero incoherent part ($\gamma_1 \neq 0$) the real component of the mobility in Equation (36) does not vanish at high frequency, in contrast to the Drude type mobility. Equations (36) and (37) were obtained for very short correlation time between the fluctuations. Correlations between fluctuations have been taken into account by replacing the Dirac δ-function in Equations (34) and (35) with an exponential function ($\delta(t) \to \tau_c^{-1}\exp(-t/\tau_c)$), which is important if $J\tau_c/\hbar$ is not a small quantity.[130–133] The latter has been used in a theoretical study of the charge carrier mobility in a columnar π-stacked triphenylene derivative.[131]

In the presence of static structural defects which hinder charge transport, the mobility will usually increase with frequency and become constant at higher frequency. This is due to the fact that at low frequencies the charges must overcome the barriers caused by the static defects in order to follow the oscillating electric field. At higher frequencies the charges do not encounter the static defects during a period of the oscillating electric field and the mobility varies with frequency due to dynamic fluctuations [*e.g.* according to Equation (36)]. The frequency dependence of the mobility of charge carriers performing normal Gaussian diffusive motion between infinitely high barriers has been treated theoretically in Refs.[37,134,135]

The temperature dependence of the mobility of charge carriers in systems with both static and dynamic disorder and weak electron–phonon coupling is not straightforward. An increase of the temperature will usually lead to fluctuations in the site energies, which reduces the mobility. On the other hand, at elevated temperature enhanced structural fluctuations may lead to smaller and/or larger values of the charge transfer integrals. The net effect of these fluctuations on the mobility

depends on the details of the system. In terms of Equation (37) an increase of γ_1 with temperature will lead to a decrease of the mobility as it is mainly determined by the coherent part [second term between square brackets in Equation (37)]. However, for high $\gamma_1$the incoherent part can become dominant and then the mobility increases with γ_1 and temperature.

2.4. *Hopping models for localized charges in strongly disordered materials*

In a material with static structural disorder the mutual arrangement of molecular units varies from one site to another. The different local environment for each molecular unit causes the polarization energy and consequently the site energy in Equation (30) to exhibit static disorder. In addition, variations in the mutual orientation of adjacent molecular units leads to static disorder in the charge transfer integrals. If the disorder in the site energy exceeds the values of the charge transfer integrals the charge carrier becomes localized and charge transport occurs by hopping between the molecular units. Two extreme different modes for hopping transport can be distinguished, either (1) phonon-assisted hopping without polaronic effects or (2) polaronic hopping of a charge carrier, which carries along a lattice deformation around itself.[99] In mode (2) the charge carrier relaxes energetically by inducing a geometrical distortion to form a so-called small polaron. For recent reviews on theoretical modelling of charge transport by hopping in molecular organic materials, see references.[81,136,137]

Hopping in the absence of polaronic effects is usually treated in terms of Miller–Abrahams hopping,[71,138–140] which is a special case of the more general Holstein–Emin equation.[99,141] The Miller–Abrahams hopping rate is valid for hopping steps upward or downward in energy by absorption or emission of a single acoustic phonon at temperatures well below the Debye temperature. The Miller–Abrahams rate for hopping from an initial site i with energy ε_i to a final site f with energy ε_f is usually expressed as

$$w_{if} = w_0 \exp\left(-2\alpha R_{if}\right) \begin{bmatrix} \exp\left(-\left(\varepsilon_f - \varepsilon_i\right)/k_B T\right) & \varepsilon_f > \varepsilon_i \\ 1 & \varepsilon_f \leq \varepsilon_i \end{bmatrix}. \tag{38}$$

With w_0 a pre-factor which is proportional to the square of the magnitude of the charge transfer integral, R_{if} the distance between the initial and final sites and α a decay factor, which takes into account the decay of the charge transfer integral with distance. Note that effects of the mutual arrangement of molecular units on the charge transfer integral other than the distance R_{if} are not included in the expression for Miller–Abrahams rate in Equation (38). Hopping steps upward in energy are thermally activated, since such steps require availability of a phonon to be absorbed. Downward steps involve emission of a phonon and are temperature independent. As discussed by Mott the hopping rate is determined by a competition between the two exponential factors in Equation (38).[142] At a small distance the first exponential factor in Equation (38) is large, but the chance of finding sites that are close in energy is small. Hence, the rate of hopping between sites at larger distance that are closer in energy to that of the initial site can be higher than for hopping between nearest neighbours. This gives rise to so-called variable range hopping in which the charge carrier makes hops between sites for which the rate is highest. The pre-factor w_0 depends on the difference

in site energies and the variation of the charge transfer integral from site to site, which are commonly ignored in modelling studies of charge transport based on Miller–Abrahams hopping. Reasoning from first principles, the applicability of the Miller–Abrahams hopping rate to organic materials is questionable, since it is restricted to charge hopping associated with single acoustic phonon transitions only and it neglects polaronic effects. The Miller–Abrahams rate should merely be considered as a phenomenological expression for the hopping rate.

In the presence of a charge induced lattice deformation the hopping rate of a charge carrier can be described by the Marcus or small polaron theory.[97,105,108,143,144] In this theory it is assumed that the charge carrier couples with harmonic nuclear vibrations. The coupling is taken into account as a linear change of the site energy with one or more (normal) vibrational coordinates. The presence of a charge at a molecular unit leads to a change of the equilibrium value of the vibrational coordinates. The energy needed to make a transition from the equilibrium geometry for the charge at the initial site to the equilibrium geometry for the charge at the final site (while the charge remains at the initial site) is the reorganization energy λ, see Section 3. The precise form of the expression for the polaron hopping rate depends on the frequencies of the nuclear vibrations, which are coupled to the charge carrier. Details of the derivation from a general expression for the polaron hopping rate to formulations for different temperature regimes have been provided by Jortner and Bixon[145,146] and Schatz and Ratner.[105] The discrete high-frequency vibrational modes are characterized by a single high frequency (intramolecular) vibrational mode with frequency ω_0. The low frequency (medium or intermolecular) modes are represented by a single frequency ω_m. In the low temperature limit, $k_BT \ll \hbar\omega_m \ll \hbar\omega_c$, the polaronic hopping rate is then given by[145,146]

$$w_{if} = \frac{2\pi|J_{if}|^2}{\hbar}\frac{\exp(-S_m - S_c)}{\hbar\omega_m}\sum_{n=0}^{n_{\max}}\frac{S_m^{p(n)}S_c^n}{[p(n)!n!]} \tag{39}$$

with $p(n) = \mathrm{Nint}((\varepsilon_f - \varepsilon_i + n\hbar\omega_c)/\hbar\omega_m)$ and $\mathrm{Nint}(x)$ the integer closest to x. The Huang–Rhys factors for low- and high-frequency modes are given by $S_m = \lambda_m/\hbar\omega_m$ and $S_c = \lambda_c/\hbar\omega_m$, respectively, with λ_m and λ_c the reorganization energies. The first factor in Equation (39), $2\pi|J_{if}|^2/\hbar$, is an electronic tunnelling term for charge transfer from the initial to the final site. The second factor accounts for the squared Franck–Condon overlap between the vibrational wavefunctions of the initial and final states, weighted by the density of final states. Note that the rate in Equation (39) is independent of temperature. In the high temperature limit, $k_BT \gg \hbar\omega_c \gg \hbar\omega_m$, the classical result originally derived by Marcus[143] is obtained[145,146]

$$w_{if} = \frac{2\pi|J_{if}|^2}{\hbar}\sqrt{\frac{1}{4\pi\lambda k_BT}}\exp\left(-\frac{(\varepsilon_f - \varepsilon_i + \lambda)^2}{4\lambda k_BT}\right) \tag{40}$$

with the total reorganization energy $\lambda = \lambda_m + \lambda_c$. The high temperature limit is often not strictly valid for molecular organic materials, since the charge may couple with high-frequency modes, due to *e.g.* intramolecular stretch vibrations, with vibrational quanta of the order of tenths of an eV, which largely exceeds k_BT. Often the energy of the intramolecular vibrational quanta exceeds the thermal energy, which is higher than the energy of the low-frequency modes; *i.e.* $\hbar\omega_c \gg k_BT \gg \hbar\omega_m$. In this case a combination of a

quantum mechanical treatment of the high-frequency mode and a classical description of the low-frequency mode is appropriate, which yields[145,146]

$$w_{if} = \frac{2\pi |J_{if}|^2}{\hbar} \sqrt{\frac{1}{4\pi\lambda_m k_B T}} \sum_{n=0}^{\infty} \exp(-S_c) \frac{S_c^n}{n!} \exp\left(-\frac{\left(\varepsilon_f - \varepsilon_i + \lambda_m + n\hbar\omega_c\right)^2}{4\lambda_m k_B T} \right). \quad (41)$$

Note that the expressions for the hopping rates given above were derived under the assumption of zero spatial overlap of the initial and final state. The effect of non-zero spatial overlap can usually to a good approximation be taken into account by using the effective charge transfer integral for J_{if}. The polaronic hopping rate in the classical limit given by Equation (40) is maximum when the energy difference $\Delta_{if} = \varepsilon_f - \varepsilon_i = -\lambda$. The rate decreases as Δ_{if} becomes higher or lower. A decrease of Δ_{if} for $\Delta_{if} < -\lambda$ leads to a decrease of the hopping rate. This is the so-called Marcus inverted region. Such a decrease of the hopping rate for negative Δ_{if} is completely absent in the Miller–Abrahams model. At low temperatures the polaronic hopping rates in Equations (40) and (41) will increase with temperature, since the temperature dependence of the exponential factor dominates. At higher temperatures the exponential factor becomes close to one and the rate decreases with temperature due the $T^{-1/2}$ pre-factor.

In case all site energies and charge transfer integrals in a material are the same the mobility of charge carriers moving by hopping with a rate w between molecular units at distance a is equal to

$$\mu = \frac{e}{k_B T} w a^2. \quad (42)$$

In a disordered material the hopping rates vary from site to site, due to variations in the site energies and charge transfer integrals. Consequently, for disordered systems, general analytical expressions for the mobility based on the hopping rates discussed above cannot be given. Theoretical evaluation of the individual site energies and mutual arrangements of different molecular units in a disordered material is a difficult and highly demanding task. Therefore, the distribution of site energies has often been taken to be a Gaussian function with a width that is considered as an adjustable parameter to achieve agreement with experimental results on charge transport. Distributions of site energies that are spatially uncorrelated[147–149] or correlated[150,151] have been used. Charge transport in disordered organic polymers has been described on the basis of Miller–Abrahams hopping rates using an analytical effective medium approach (EMA),[99,152,153] a master-Equation approach,[148] or by Monte Carlo computer simulations.[147,154–159] The values of w_0, R_{if} and α in Equation (38) for the Miller–Abrahams hopping rate were estimated or treated as adjustable parameters. Recent theoretical studies of charge transport by polaronic hopping have incorporated more details of effects of structural fluctuations on charge transfer integrals and site energies, while reorganization energies were obtained from quantum chemical calculations. In recent years computational studies of polaronic hopping transport have been carried out for a variety of molecular materials, including oligoacenes,[160] polymers,[148,158,161,162] π-stacked molecular materials[163–165] and DNA.[127]

Other hopping models involving thermally activated jumps out of potential wells or over barriers with a Gaussian or exponential distribution of the energies have also been studied.[166–169] Charge transport along columns of π-stacked derivatives of triphenylene molecules could be successfully described by hopping over barriers.[170] It has been pointed

out that the Einstein relation between mobility and the diffusion coefficient is violated for hopping in a disordered energy landscape with different site energies, prior to full thermal relaxation of the charge carriers.[171] Hopping of charge carriers in an energetic landscape with different barriers causes the mobility to increase with the oscillation frequency of the applied electric field.[76,154,168] This can be understood as follows: at higher frequency the charges move for a shorter time, and consequently a shorter distance, during an oscillation period of the field. Therefore, at higher frequency it is less likely that a charge encounters a barrier during the oscillation period of the field. This leads to an increase of the mobility with frequency. At sufficiently high frequency the charges can just move between the barriers to follow the oscillating field direction and the mobility attains a maximum value.

3. Calculation of parameters involved in charge transport

To perform calculations of the charge carrier mobility on the basis of the models described in Section 2, the site energies, ε, charge transfer integrals, J, and spatial overlap, S, integrals must be known. In the case of polaronic hopping transport knowledge of the reorganization energy is also required. To calculate ε, J, and S the wavefunctions, φ, in Equation (8), which describe the charge at the different molecular units in the system, must be specified. It has been common practice in studies reported in the literature to proceed from the molecular orbitals for neutral molecular units. This is appropriate if charges are sufficiently delocalized so that the amount of charge on a molecular unit is so small that charge induced orbital relaxation can be neglected. However, for strongly localized charge carriers use of orbitals for charged molecular units may be more appropriate.

In what follows, methods to compute ε, J, and S on basis of wavefunctions (φ) for neutral molecular units will be considered. The values of J and S for charge transfer between adjacent molecular units A and B can be obtained by considering a system consisting of A and B only. Site energies for holes and excess electrons can, to a first approximation, be taken equal to the ionization energy and the electron affinity of the molecular units, respectively. However, the site energy at a particular molecular unit A will be affected by the presence of surrounding molecular units. Hence, to obtain accurate values of the site energies these surrounding molecular units must be included in the calculations. As an example, the site energy of a nucleobase in DNA strongly depends on the nature of neighbouring nucleobases, which in turn leads to a strong sequence dependence of oxidative damage in DNA.[127,172]

The charge transfer and spatial overlap integrals are matrix elements involving the many electron wavefunction describing an excess charge at molecular unit A and the wavefunction for the charge at unit B. The many electron wavefunction for the neutral composite system AB can be written as an antisymmetrized product (Slater determinant)[173] of the occupied molecular spin orbitals on the molecular units A and B. The wavefunction φ_A describing an excess electron on unit A is obtained by introduction of an excess electron spin orbital on unit A to the many electron wavefunction of the neutral system AB. The wavefunction for an excess electron on unit B is obtained analogously. The excess electron orbital can in a first approximation be taken as the LUMO for the neutral molecular unit. The many electron wavefunction for a hole on unit A is obtained by removing a HOMO spin orbital on unit A from the Slater determinant for the neutral composite system AB. The wavefunction for a hole on unit B is obtained analogously.

The many electron wavefunctions for an excess charge on units A and B thus differ by one molecular spin orbital: for excess electrons this difference corresponds to the occupation of the LUMO on unit A or on unit B, while for holes this is the occupation of a HOMO on unit A or on unit B. Provided that all molecular spin orbitals other than these LUMO and HOMO orbitals are orthonormal, the Slater matrix rules[173] can be applied to obtain the matrix elements of the Hamiltonian and the spatial overlap integral. The charge transfer integral is then equal to the matrix element

$$J_{AB} = \langle A|h|B\rangle \tag{43}$$

with h the Hartree–Fock operator or the Kohn–Sham operator in density functional theory (DFT) for the composite system AB and A and B the HOMO or LUMO orbitals of the individual molecular units A en B, respectively. The spatial orbital overlap integral of the many electron wavefunctions for a charge at units A and B is equal to

$$S_{AB} = \langle A|B\rangle. \tag{44}$$

Analogous to Koopman's theorem[173] the site energy of a charge at molecular unit A can be calculated as the diagonal matrix element of the h operator for a system consisting of molecular unit A and all surrounding molecular units that affect the site energy on A; *i.e.*

$$\varepsilon_A = \langle A|h|A\rangle. \tag{45}$$

The results of Equations (43)–(45) can be used to calculate the effective charge transfer integral according to Equation (15), which can be used in subsequent calculations in which the spatial overlap no longer needs to be taken into account, explicitly.

A direct way to obtain the site energies and the charge transfer and overlap integrals is to first compute the molecular orbitals for individual molecular units with an atomic orbital basis set. The molecular (*not atomic*) orbitals obtained for the individual molecular units should then be used as basis functions in a subsequent electronic structure calculation on the composite system of two or more molecular units. The matrix elements of the h-operator in the latter calculation correspond to the site energies and charge transfer integrals, while the spatial overlap can be obtained in a straightforward manner. It should be noted that, one can use atomic orbitals in the calculation on the composite system and subsequently carry out a transformation from the atomic orbital basis to the basis of the molecular orbitals on the individual molecular units.[174] However, this is less convenient than directly using molecular orbitals as a basis set.

Direct calculation of the matrix elements in Equations (43) to (45) can be realized by exploiting the unique feature of the Amsterdam Density Functional theory program[175] (ADF) that allows one to use molecular orbitals as a basis set in electronic structure calculations on a system consisting of different molecular units. First the molecular orbitals for the individual molecular units are calculated with an atomic basis set. These molecular orbitals are then used as a basis set in a subsequent electronic structure calculation on a system composed of two or more molecular units. The standard output of the ADF program then provides the overlap matrix, **S**, the eigenvector matrix, **C**, and the diagonal eigenvalue matrix, **E**, defined in terms of the molecular orbitals on the molecular units. The matrix elements of the Kohn–Sham Hamiltonian, $\langle\varphi_A|h_{KS}|\varphi_B\rangle$, can be readily obtained from **S**, **C** and **E**, since $\mathbf{h_{KS}C} = \mathbf{SCE}$, and consequently $\mathbf{h_{KS}} = \mathbf{SCEC}^{-1}$. The 'fragment orbital procedure' (FO-procedure) described above allows direct calculations of

the charge transfer integrals, including their signs, without invoking the assumption of zero spatial overlap. Note that the sign of the site energy and the charge transfer integral for a description of hole transport is opposite to that of the corresponding matrix elements of the *h*-operator involving the electronic orbitals of the missing electron. The ADF program has been applied to calculate site energies and charge transfer integrals according to the FO-procedure described above for discotic π-stacked materials,[93,163,164,176] conjugated polymers[82,85,96,177] and DNA.[127,172]

Charge transfer integrals have often been calculated using the so-called energy-splitting-in-dimer (ESD) method in which the charge transfer integral is obtained from the energetic splitting between the HOMOs or LUMOs in a system consisting of two molecular units.[81,174] For a symmetric dimer consisting of two identical molecular units and zero spatial overlap the charge transfer integral is equal to half the HOMO or LUMO splitting (provided the HOMO and LUMO on one molecule only couples with the corresponding orbital on the other molecule). In the case of non-zero spatial overlap the orbital splitting in a symmetric dimer is approximately equal to the effective charge transfer integral in Equation (15).[81,93] In a non-symmetric dimer (hetero-dimer) the site energies of the two molecular units differ from each other and the (effective) charge transfer integral can no longer be directly obtained from the orbital splitting in the dimer only. In such a case approximate site energies can be obtained from a calculation of the orbital energies for an individual molecule in the field of the other molecule, with the latter being represented by point charges.[81,92] The effective charge transfer integral is then calculated from these site energies and the orbital splitting in the hetero-dimer. Another method that has been applied to obtain the effective charge transfer integrals for nucleobases in DNA involves application of an external electric field to bring the site energies of different molecular units into resonance.[178–181] Compared with the methods based on the orbital splitting in a dimer, the FO-procedure carried out with the ADF program has several advantages. The FO-procedure is more direct and exact and it can also be used for hetero-dimers (or larger systems) in which orbitals on one molecular unit interact with different orbital on another unit.[93] This occurs for instance for triphenylenes and hexabenzocoronenes for which the HOMO's and LUMO's are twofold degenerate.[93,163] Note, that the value of the calculated charge transfer integral may depend on the method (Hartree–Fock, DFT) used for the electronic structure calculations. Charge transfer integrals calculated with DFT and Perdew–Wang functionals were found to agree better with experimental bandwidths for some organic molecules and graphite than Hartree–Fock.[174]

The reorganization energy, λ, in Equations (40) and (41) is in general due to charge induced structural rearrangement of the molecular unit containing the charge and due to reorganization of the surrounding medium.[105,182] These two contributions are referred to as the internal and external reorganization energy, respectively. The reorganization energy for charge transfer from an initial site to a final site is the energy needed for rearrangement of the nuclei from the equilibrium geometry for the charge at the initial site to the equilibrium geometry for the charge at the final site, with the charge remaining localized at the initial site. The reorganization energy can be expressed as[183]

$$\lambda = \left[E^q(g^0) - E^q(g^q)\right] + \left[E^0(g^q) - E^0(g^0)\right] \tag{46}$$

where $E^q(g^0)$ is the energy of the system with an excess charge $q = \pm 1$, while the nuclear geometry (g^0) corresponds to that for the neutral system at equilibrium, etc. For the internal reorganization energy for hole (electron) transfer the term $E^q(g^0)$corresponds to the energy of a cation (anion) with the equilibrium geometry of a neutral molecular unit. The other terms in Equation (46) are defined analogously. Internal reorganization energies can be obtained from Hartree–Fock, DFT or Mller–Plesset perturbation theory.[173] The reorganization energy often depends significantly on the theoretical method used. For oligoacene molecules the Hartree–Fock method has been found to overestimate charge induced structural deformations and reorganization energies.[184] A localized excess charge in a molecular organic solid will mainly cause a distortion of the molecular unit at which it resides, while structural reorganization of the environment will be relatively small. In such a case the reorganization energy can to a good approximation to be taken equal to the internal reorganization energy.

Site energies and charge transfer integrals usually depend strongly on the mutual arrangement of the molecular units in a material. Therefore, accurate information on the arrangement and dynamics of the molecular units is essential. Such information can be obtained theoretically from molecular mechanics and molecular dynamics simulations.[163,165]

4. Discussion of experimental results

4.1. *Discotic materials*

As discussed in Section 1, liquid crystalline discotic materials consist of molecules with a flat aromatic central core and flexible peripheral side chains (see Figure 4). Discotic molecules can self-organize by stacking on top of each other, so that columnar aggregates are formed. The electronic π-orbitals on adjacent molecules within a column overlap and in this way a one-dimensional pathway for charge transport is realized along the column. Within the class of columnar liquid crystalline discotic materials, triphenylene derivatives are one of the most studied materials, with respect to both structural and charge transporting properties.[53,185–188] The focus of this section is on triphenylene derivatives. At lower temperatures triphenylene derivatives exhibit a crystalline phase, with a relatively high degree of structural order. On increasing the temperature (typically a few tens of degrees K above room temperature) one or more liquid crystalline phases are encountered in which the aliphatic side chain substituents exhibit liquid-like fluctuations. At higher temperatures an isotropic liquid phase is reached where the columnar order has disappeared. Experimental[189–196] and theoretical[197–199] studies on the structure of liquid crystalline triphenylene derivatives have revealed that the average intracolumnar stacking distance is close to 3.5 Å, while the twist angle is between 45 and 60 degrees. The values are averages and it is important to realize that structural fluctuations in the form of longitudinal oscillations, twisting motion and lateral slides of the molecules are significant (see Figure 7).

The mobility of charge carriers in these materials is of particular relevance to their possible use in opto-electronic device applications.[53,186,187] Charge transport along the columnar direction is facilitated by the electronic coupling between the electronic π-orbitals on adjacent molecules within the same column. The aromatic cores of the discotic molecules in different columns are separated by long aliphatic side chain

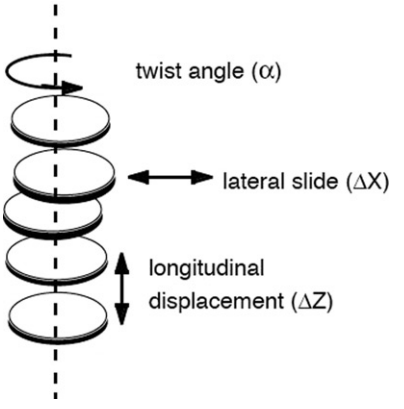

Figure 7. Schematic representation of columnar stacked triphenylene molecules with disorder in the form of different twist angles (α), stacking distance (ΔZ), and lateral slide motion (ΔX).

substituents, which is unfavourable for charge transport from one column to another. Indeed the mobility of charge carriers along the columnar direction has been found to be about three orders of magnitude higher than the mobility for charge transport perpendicular to the columns.[200–202] Experimental mobility values for intracolumnar charge transport have been obtained from time-of-flight (TOF) measurements,[203–215] pulse-radiolysis time-resolved microwave conductivity (PR-TRMC) measurements,[50,61,170,216–221] and frequency dependent AC conductivity measurements on doped samples.[201,202,222,223] In earlier TOF studies on triphenylene derivatives only mobile holes were observed, due to fast scavenging of excess electrons on trace amounts of impurities such as oxygen.[186,215] Indeed, in sufficiently pure samples ambipolar charge transport has been observed with electron and hole mobilities of comparable magnitude.[213–215] Mobilities for holes and electrons in the range 10^{-3}–$10^{-2}\,cm^2\,V^{-1}\,s^{-1}$ have been reported for alkoxy-substituted triphenylenes in the liquid crystalline phase. The disperse photocurrent transients and frequency dependence of the charge carrier mobility indicate that structural disorder affects charge transport.[170,201,202,222,223] As discussed in Sections 2.1 and 2.4 a frequency dependence of the charge carrier mobility can be caused by barriers to charge transport, resulting from structural disorder in the material. Interestingly, for hexakis-hexylthiotriphenylene (HHTT) in its liquid crystalline phases the DC mobilities obtained from TOF measurements and the AC mobilities at a microwave frequency of 30 GHz from PR-TRMC measurements are similar. Apparently, for HHTT disorder plays a much smaller role than for alkoxy-substituted triphenylenes.[217] The reduced effect of disorder for HHTT agrees with the relatively high charge carrier mobility of $0.1\,cm^2\,V^{-1}\,s^{-1}$ in the liquid crystalline H-phase. In the crystalline K-phase of HHTT the microwave mobility was found to be as high as $0.3\,cm^2\,V^{-1}\,s^{-1}$.[217]

For both alkoxy- and alkylthio-substituted triphenylenes the microwave mobility is highest in the crystalline K-phase. In the K-phase the materials are polycrystalline and grain boundaries act as barriers for charge transport over longer distances. This hampers the determination of mobility values from TOF measurements, where charges need to traverse the entire sample between the electrodes at a distance of typically a few tens of

micrometers. The mobility usually decreases abruptly with temperature at the transition to the liquid crystalline phase. On further heating to the isotropic liquid phase the mobility values exhibit a further sudden decrease to values below the experimental detection limit.[50] The width of the temperature range of the liquid crystalline phase is about 50 K. Measurements over this temperature range on the liquid crystalline phase and measurements over a comparable range on the crystalline phase have yielded mobility values that do not vary much with temperature. Different theoretical models have been applied to explain the almost temperature independent mobility.[131,211,224] However, conclusions based on the lack of a strong temperature dependence over these very limited ranges should be taken with caution. In this context it is of interest to consider the combination of DC and AC mobility measurements on a triphenylene dimer, which exhibits a plastic liquid crystalline phase over a large temperature range between 130 K and 400 K. The DC mobility obtained from TOF measurements increases with temperature over this range by almost four orders of magnitude from $2 \times 10^{-6}\,cm^2\,V^{-1}\,s^{-1}$ to[170] $0.01\,cm^2\,V^{-1}\,s^{-1}$. Between room temperature and 410 K the DC mobility was found to be almost constant. This shows that the mobility can be strongly thermally activated at lower temperatures, while it turns out to be close to constant at higher temperatures where most triphenylene derivatives exhibit their liquid crystalline phase. Interestingly, the AC microwave mobility for the triphenylene dimer was almost temperature independent over the entire range between 170 K and 400 K. The temperature dependence of the DC and AC mobilities could be explained with a phenomenological theoretical model for thermally activated hopping of charges in a disordered energy landscape with barriers with a mean height of[170] 0.024 eV.

As discussed in Sections 2 and 3, a theoretical description of the charge carrier mobility requires information about the charge transport parameters as a function of the (dynamical) geometric conformation of the molecules in the material. Charge transfer integrals for hole transport have been estimated from band structure calculations[131] and from the energy-splitting-in-dimer (ESD) method.[221,225] As discussed in Section 3, the latter is only correct for a symmetric dimer system in which the two molecules are equivalent and for the case of zero spatial overlap between the orbitals on different molecules. These conditions are not applicable to disordered stacks of triphenylene derivatives. Therefore charge transfer integrals and site energies have been calculated according to the FO-procedure described in Section 3. The results of these calculations are discussed below and details can be found in Ref.[93]

Charge transport of holes can, to a good approximation, be described on basis of the HOMO orbitals. The HOMO orbitals of a triphenylene molecule are twofold degenerate. A perfectly ordered columnar stack of triphenylene molecules with the molecular planes perpendicular to the stacking axis and the centres of mass on this axis has C_3 symmetry. In this case symmetry adapted linear combinations (SALCs) of the orbitals on the individual molecules can be made, such that each HOMO on a particular molecule couples only with one orbital on an adjacent molecule. The charge transfer and spatial overlap integrals for symmetry adapted HOMOs are complex numbers.[93] In case of structural disorder the C_3 symmetry will be broken and each HOMO on one triphenylene molecule will interact with both HOMOs on an adjacent molecule. In the calculations on systems consisting of two stacked triphenylene molecules the HOMO in the dimer was found to be composed of the HOMOs on the individual molecules by

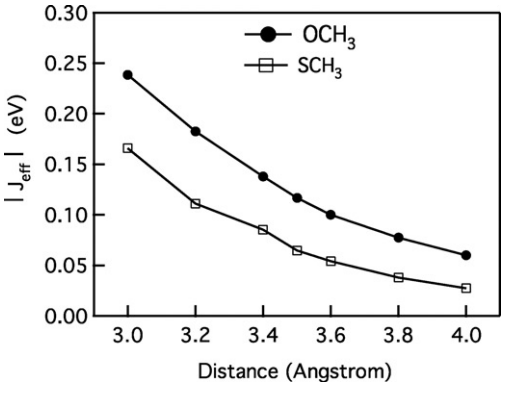

Figure 8. Distance dependence of the absolute value of the effective charge transfer integrals for methoxy- and methylthio-substituted triphenylenes at a twist angle of 45 degrees.

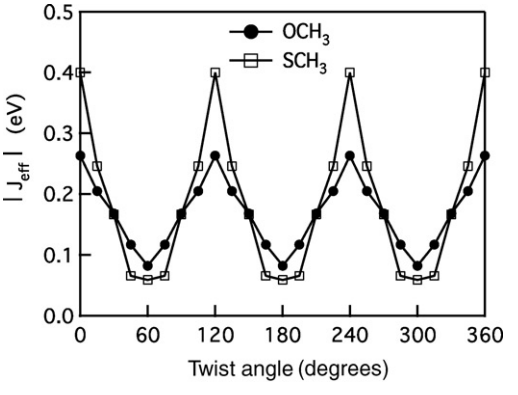

Figure 9. Variation of the absolute value of the effective charge transfer integral with the twist angle for methoxy- and methylthio-substituted triphenylenes with a stacking distance of 3.5 Å.

more than 98%. The description of a positive charge carrier in terms of the HOMOs only can thus be considered adequate.

Figure 8 shows the dependence on longitudinal displacement (ΔZ in Figure 7) of the absolute value of the effective charge transfer integrals, $|J_{eff}|$ in Equation (15), for methoxy- and methylthio-substituted triphenylenes. The calculations were performed for the (equilibrium) twist angle of 45 degrees. At this twist angle the charge transfer integral is highest for methoxy-substituted triphenylene. The variation of the magnitude of the effective charge transfer integrals with the twist angle ($\delta\alpha$ in Figure 7) is shown in Figure 9. The charge transfer integrals exhibit a large variation with the twist angle with the effect being strongest for methylthio-substituted triphenylene. This indicates that motion of charges will be significantly affected by the twist angles in the material. Figure 10 shows the absolute values of the charge transfer integrals as a function of the lateral slide distance (ΔX in Figure 7) for methoxy-substituted triphenylene. The twist angle was taken equal to

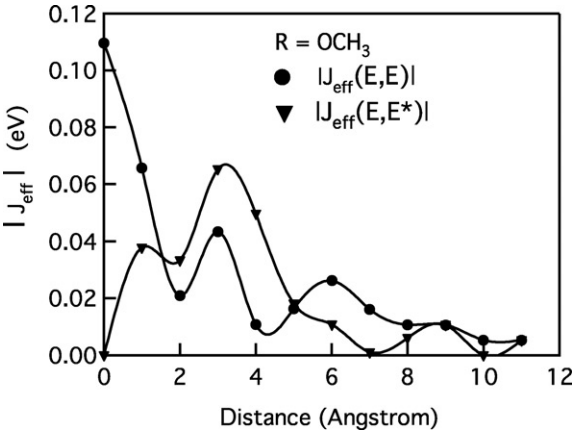

Figure 10. Dependence of the absolute values of the effective charge transfer integrals on the lateral slide distance for methoxy-substituted triphenylene molecules with a stacking distance of 3.5 Å and a twist angle of 45 degrees.

45 degrees. Similar results were found for 60 degrees twist and for methylthio-substituted triphenylene. For zero lateral slide distance the system has C_3 symmetry and consequently the charge transfer integral involving inequivalent HOMOs on one molecule and the other, $J_{eff}(E, E^*)$, is equal to zero. As the slide distance increases the charge transfer integral for equivalent orbitals on adjacent molecules, $J_{eff}(E, E)$, first decreases, then exhibits local maxima and tends to zero at distances exceeding 8 Å. The charge transfer integral involving different HOMOs on the two molecules, $J_{eff}(E, E^*)$, increases initially and then decreases. From the results in Figure 10 it can be concluded that lateral displacements of ~8 Å or more will have a large negative effect on the mobility of charge carriers.

In triphenylenes fluctuations of the twist angles and intermolecular distance of the order of 50 degrees and 1 Å have been estimated.[131] The data discussed above shows that such fluctuations could lead to significant variations of the charge transfer integrals. In addition, the occurrence of large lateral displacements causes the charge transfer integral to become small and will have a strong negative effect on the charge carrier mobility. These fluctuations were also found to lead to variation of the site energies on the order of 0.1 eV. In addition, internal vibrational modes of the aromatic core lead to variations of the charge transfer integral and site energy on the order of 0.1 eV.[198] Hence, fluctuations of the site energy can exceed the value of the charge transfer integral. In case the fluctuations occur on a timescale, which is short compared to charge motion from one molecule to another, the methods in Section 2.3 are appropriate to describe charge transport with Equations (36) and (37) applicable to the case of very fast fluctuations. Slower fluctuations can lead to charge localization and transport via hopping, as discussed in Section 2.4. Realization of structurally ordered stacks of triphenylenes is expected to have a large positive effect on the charge carrier mobility. Since the charge transfer integral is higher for smaller twist angle (see Figure 9) a reduction to values near zero degrees, *e.g.* by using different substituents, can further enhance the mobility significantly. A relatively high charge carrier mobility

has indeed been found for H-bond-stabilized triphenylenes with a small mutual twist angle near 15 degrees.[61]

Internal reorganization energies for triphenylene derivatives have been calculated at the DFT level according to Equation (46).[163] For alkoxy-substituted triphenylene the reorganization energies are $\lambda_+ = 0.33\,\text{eV}$ for a hole and $\lambda_- = 0.40\,\text{eV}$ for an excess electron. For alkylthio-substituted triphenylene these values are about a factor two smaller; *i.e.* $\lambda_+ = 0.16\,\text{eV}$ and $\lambda_- = 0.24\,\text{eV}$.

The data in Figures 8–10 show that the effective charge transfer integral has a magnitude of about 0.1 eV near the equilibrium arrangement of adjacent molecules. Hence, the reorganization energies mentioned above do not exceed the charge transfer integral to a very large extent. In particular, taking into consideration that the charge transfer integral increases for fluctuations of the twist angle to smaller values, it is not obvious whether or not a small polaron is formed with charge transport taking place via hopping with a rate given in Equation (39), (40) or (41). Theoretical models for incoherent hopping[163,170,225] or (partially) coherent band like motion[131,221,224,226] with effects of dynamic or static structural fluctuations have been used to describe charge carrier mobilities in triphenylene derivatives. Until now the mechanism of charge transport in discotic liquid crystalline materials has not been established.

The mobility of charge carriers would attain a maximum value in the hypothetical case of perfectly ordered molecular stacks and in the absence of polaronic effects. In this case the band model of Section 2.2 would be applicable. The charge transfer integral of 0.1 eV exceeds thermal energy so that triphenylene stacks can then be considered as one-dimensional wide band gap semiconductors, as described in Section 2.2.1. According to Equation (20) a charge transfer integral of 0.1 eV corresponds with an effective mass equal to 3 times the free electron mass. This value is about one order of magnitude higher than for holes in Si or III-V semiconductors (*e.g.* GaAs), for which typical hole mobilities are in the range $100–1000\,\text{cm}^2\,\text{V}^{-1}\,\text{s}^{-1}$.[227] Assuming a similar scattering time (of the order of 100 fsec) in ordered triphenylene stacks and inorganic semiconductors, Equation (23) yields a mobility of $10–100\,\text{cm}^2\,\text{V}^{-1}\,\text{s}^{-1}$ for the former. This estimated mobility for ordered triphenylene stacks is similar to the experimental values for crystals of oligoacenes such as pentacene[25] and rubrene.[26,27] Interestingly, the charge transfer integrals and reorganization energies for triphenylenes discussed above are similar to those calculated for oligoacene crystals,[228] which suggests that mobilities of $10–100\,\text{cm}^2\,\text{V}^{-1}\,\text{s}^{-1}$ can indeed be realized for structurally ordered triphenylene stacks. In case charge transport would occur by polaronic hopping in the classical limit, Equations (40) and (42) can be used to estimate the mobility. For polaronic hopping along an ordered stack of triphenylene molecules with identical site energies, a charge transfer integral of 0.1 eV and a reorganization energy of 0.2 eV, the room temperature mobility is calculated to be $1\,\text{cm}^2\,\text{V}^{-1}\,\text{s}^{-1}$. This value must be considered as a lower limit to the mobility along an ordered stack, since it is based on the assumption that the charge is fully localized on a single molecule, which only holds if the reorganization energy largely exceeds the charge transfer integral.

The fact that experimental charge carrier mobilities for triphenylene derivatives are smaller than $1\,\text{cm}^2\,\text{V}^{-1}\,\text{s}^{-1}$ immediately shows that the idealized band and polaronic hopping models discussed above are not applicable. This is not surprising since for

realistic samples charge transfer integrals and site energies will vary from one molecule to another. Effects of static and dynamic disorder on these parameters must be taken into account, which will lower the calculated mobility. To this end, detailed information about the material structure and fluctuations thereof is needed. Both experimental studies and molecular dynamics simulations can contribute to the latter. The degree to which structural disorder and polaronic effects induce localization of a charge carrier over one or more molecules must be established. In case charge carriers do not exhibit a large degree of localization hopping models are inadequate and charge transport can in principle be described using the general methodology of Section 2.3.

4.2. *Oligo(phenylene-vinylene) stacks*

Other interesting examples of self-organizing materials are assemblies of hydrogen-bonded dimers of phenylene-vinylene oligomers (MOPVn) (see Figure 11). In aliphatic hydrocarbon solvents these dimers self-assemble into chiral π-stacks that have been shown to be relatively efficient pathways for exciton transport.[229,230] As discussed in Section 2 the transport efficiency of charges in such stacks critically depends on the charge transfer integral for neighbouring molecules. Although the aggregates formed are relatively well ordered, the degree of organization will be considerably less than in organic molecular crystals.

The charge transport properties of fibres of π-stacked MOPVs have been investigated by depositing MOPV-stack fibres on a grid of electrodes with a spacing of 100 nm.[231] However, no current was measured through these fibres. This raises the question whether the self-assembled helical structure that is formed in solution is retained when the fibres are transferred from solution to the substrate. It has been demonstrated that the stacks can be transferred to a substrate, while preserving their internal organization.[232,233] However, it cannot be ruled out that the organization of the stacks on a substrate differs from that in solution. Moreover, in a device configuration complications can occur since the charges have to overcome the injection barriers at the contacts. In order to establish whether these self-organized π-stacks in solution provide a pathway for efficient charge transport, pulse-radiolysis time-resolved microwave conductivity experiments have been performed.[164] In these experiments it is possible to measure the mobility of charges on conjugated polymers

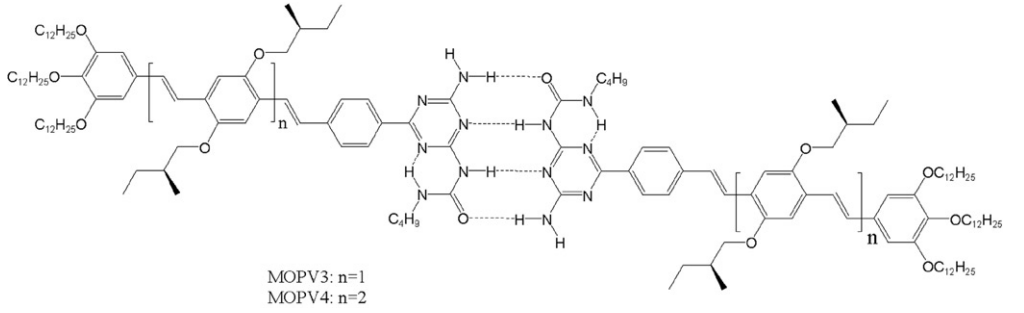

Figure 11. Structure of hydrogen bonded dimers of a phenylene-vinylene derivative (MOPV).

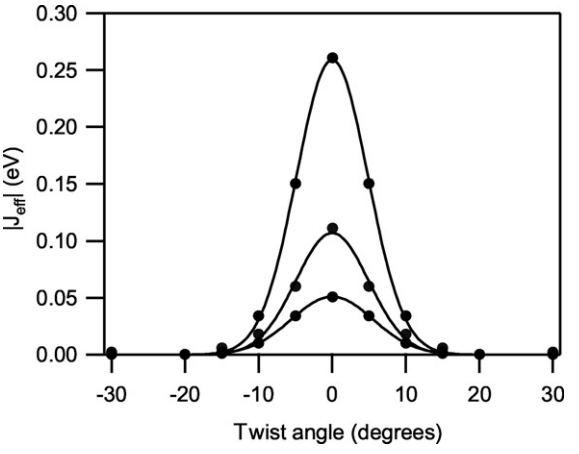

Figure 12. Dependence of the effective charge transfer integral J_{eff} on the twist angle for MOPV3 at stacking distances of 3.5, 4.0 and 4.5 Å (from top to bottom).

chains or molecular assemblies in solution.[234–236] In spite of the relatively high degree of organization of the π-stacks in solution, the mobility of charge carriers along the aggregates was found to be only $3 \times 10^{-3}\,cm^2\,V^{-1}\,s^{-1}$ for holes and $9 \times 10^{-3}\,cm^2\,V^{-1}\,s^{-1}$ for electrons.[164] In order to understand this low mobility, the relation between the organization on a molecular scale and the parameters that govern the charge transport properties has to be considered. As discussed in Section 2, two of the parameters that are of critical importance for determining the efficiency of charge transport are the charge transfer integral and the reorganization energy.

The effective charge transfer integral, J_{eff}, between stacked MOPV molecules in the same strand was found to be much larger than those for transport from one strand to another.[164] Therefore the mobility of charge carriers is determined by transport along one of the strands in a stack of MOPV dimers. The effective charge transfer integrals were calculated using the FO-procedure described in Section 3 for the HOMO and LUMO, which are the relevant orbitals for hole and electron transport, respectively. In Figure 12 the effective charge transfer integral for intrastrand hole transport is plotted for MOPV3 as a function of the twist angle for different stacking distances. The twist angle is defined as the mutual angle between two stacked dimers where the centre of mass (between the two hydrogen bonding units) is the centre of rotation. The coupling is maximal for zero twist angle where the overlap between the molecules is optimal. For all stacking distances J_{eff} rapidly decays with increasing twist angle and becomes close to zero for angles larger than 15 degrees.

The internal reorganization energies were calculated using DFT, as discussed in Section 3. For MOPV3 the internal reorganization energies were found to be 0.20 eV for the hole and 0.25 eV for the electron. For MOPV4 both reorganization energies were smaller; 0.16 eV for the hole and 0.20 eV for the electron. The smaller reorganization energies for MOPV4 reflect the more delocalized nature of the charge on the longer oligomer. The net charge per phenylene-vinylene unit is smaller for MOPV4 (see also

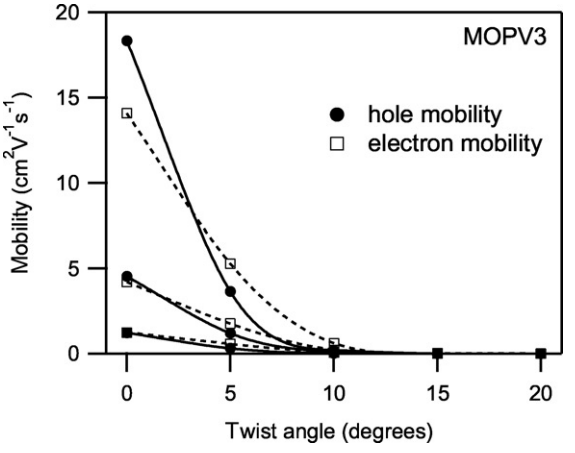

Figure 13. Dependence of the electron and hole mobility on the twist angle in stacks of MOPV3 at stacking distances of 3.5 Å, 4 Å and 4.5 Å (from top to bottom).

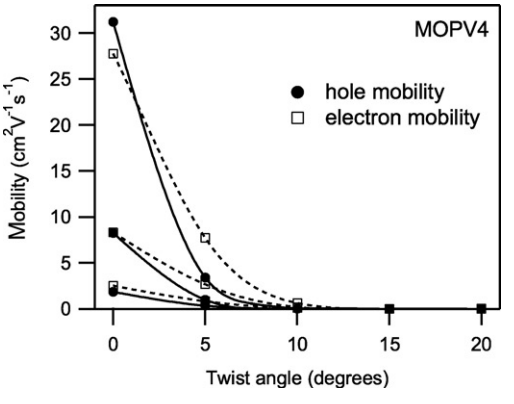

Figure 14. Dependence of the electron and hole mobility on the twist angle in stacks of MOPV4 at stacking distances of 3.5Å, 4 Å and 4.5 Å (from top to bottom).

Figure 16 for the charge distributions obtained from DFT calculations) and therefore the geometry deformations induced by the charge are less.

The effective charge transfer integrals and reorganization energies were used to calculate the charge transfer rate according to Equation (40), where the initial and final site energies are the same. The mobility of holes and electrons along stacks of MOPV3 and MOPV4 can then be calculated as a function of the twist angle and the stacking distance by using Equation (42). The results are shown in Figures 13 and 14 for MOPV3 and MOPV4, respectively. For zero twist angle a stacking distance of 3.5Å the calculated mobility of holes is $18\,cm^2\,V^{-1}\,s^{-1}$ for MOPV3 and $32\,cm^2\,V^{-1}\,s^{-1}$ for MOPV4. It is known from experiments that MOPV dimers self-assemble into a helical geometry with non-zero twist angle.[232] Increasing the twist angle from zero degrees leads to a dramatic decrease of the charge carrier mobility, which is strongest for holes. According to the

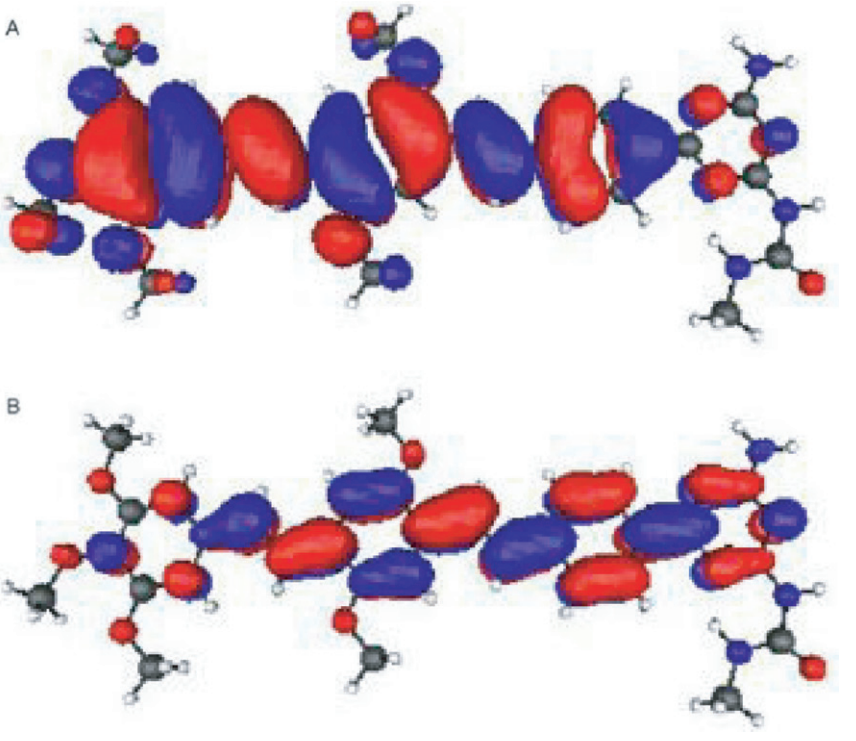

Figure 15. HOMO (A) and LUMO (B) orbitals of MOPV3.

strong decrease of the effective charge transfer integral with increasing distance (Figure 12), the charge carrier mobilities will also be affected by fluctuations of the stacking distance.

The stronger dependence of the mobility on the twist angle for the hole, as compared to that for the electron, can be understood by considering the molecular orbitals relevant for hole and electron transport. In Figure 15 the HOMO and LUMO orbitals are shown for MOPV3. The HOMO is located on the phenylene-vinylene part of the molecules with the highest density towards the end-phenyl unit that is substituted with three alkoxy-chains. The contribution of atomic orbitals on the hydrogen-bonding unit to the HOMO orbital is negligible. For the LUMO the situation is reversed; there is hardly any density on the end-phenyl unit, while there is a substantial density on the hydrogen-bonding unit. These results are consistent with previous calculations on alkoxy-substituted oligo(phenylene-vinylene)s where it was found that positive charges tend to localize on phenyl rings containing alkoxy side chains rather than on unsubstituted phenyl groups.[237] The shape of the HOMO and LUMO orbitals provides a representative picture of the charge distributions of the positive and negative charge on the MOPV chains. This can be seen in Figure 16 where the distributions of the positive and negative charge on the phenylene and vinylene units on the MOPV3 cation and anion is shown. The positive charge is localized mostly at the end-phenyl group that contains three alkoxy side chains, whereas the negative charge is mostly localized at the hydrogen-bonding unit. The spatial

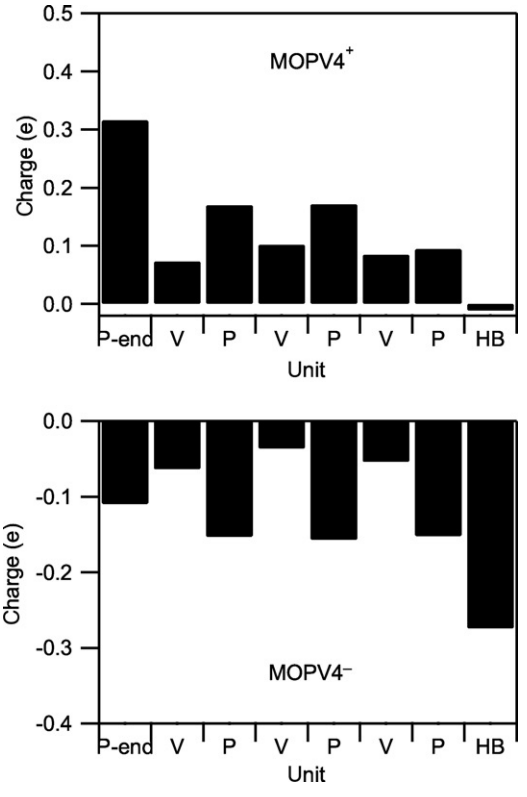

Figure 16. Charge distribution on positively and negatively charged MOPV4. P, V and HB indicate the phenylene and vinylene units and the hydrogen-bonding unit, respectively.

distribution of the charges and of the HOMO and LUMO orbitals provides insight in the origin of the difference in the angular dependence of the hole and electron mobility. The hole is localized at the chain ends, far away from the centre of rotation. This causes the overlap between the HOMO orbitals to decrease rapidly with increasing angle. The electron is localized close to the centre of rotation at the hydrogen-bonding unit. Therefore, the overlap decreases slower with increasing angle. Consequently, the hole mobility for MOPV4 decays faster with increasing angle than for MOPV3, since the localization site of the hole is further from the rotation centre for MOPV4.

In the mobility calculations discussed above, it was assumed that the stack of MOPV molecules forms a helical structure with a fixed twist-angle between neighbouring hydrogen-bonded dimers. However, the stacks will exhibit deviations from such a perfectly regular structure. In order to examine the effect of structural fluctuations on the charge carrier mobility, computer simulations of polaron hopping were performed. In the simulations dynamic fluctuations of the twist angles between neighbouring MOPV dimers were taken into account. Fluctuations in the twist angles lead to variations of the hopping rates between neighbouring MOPV4 molecules along the stack. The angles between neighbouring molecules were evenly distributed between 7 and 17 degrees, a symmetrical

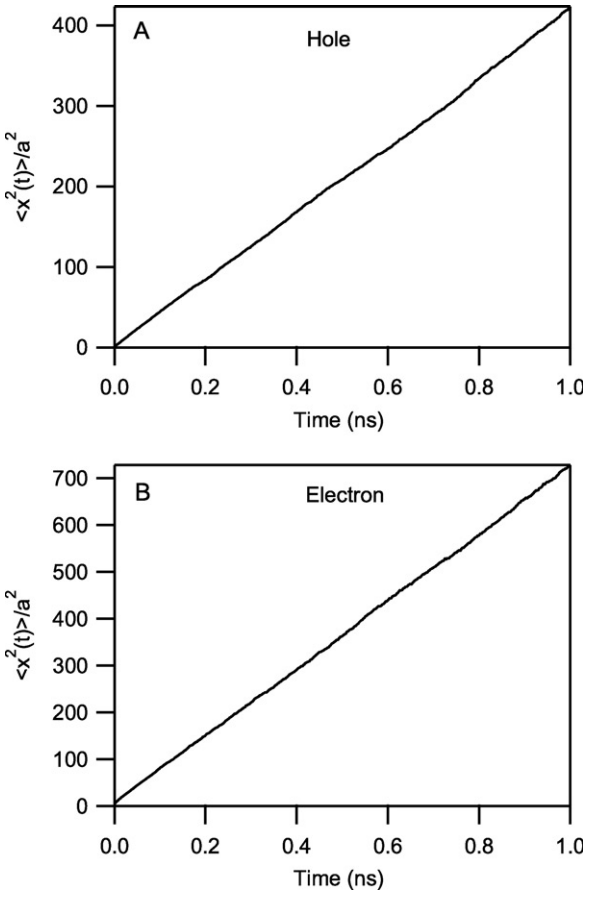

Figure 17. Calculated mean square displacement of a hole (top) and an electron (bottom) along a dynamic MOPV4 stack with a stacking distance of 3.5 Å.

interval of angles around the equilibrium angle of 12 degrees, which has been reported in reference.[232] The twisting dynamics of the MOPV dimers in the stacks was described by rotational diffusion with a rotational diffusion time of 20 ns.[164] The time dependence of the mean square displacement obtained from the simulations is shown in Figure 17. The diffusion constant, D, of the charge carrier is obtained from the slope of the curves using Equation (9) and the charge carrier mobility is calculated with the Einstein relation in Equation (10). The calculated mobility is $0.010\,cm^2\,V^{-1}\,s^{-1}$ for holes and $0.017\,cm^2\,V^{-1}\,s^{-1}$ for electrons. The calculated mobilities for twist angles fluctuating between 7 to 17 degrees is the same as the mobility for a static stack with inter-unit angles of 17 degrees. This shows that for these one-dimensional stacks the mobility is limited by the slowest hopping steps and large twist angles. The calculated mobilties are somewhat higher than the experimental values ($3 \times 10^{-3} cm^2\,V^{-1}\,s^{-1}$ for the hole and $9 \times 10^{-3}\,cm^2\,V^{-1}\,s^{-1}$ for the electron).[164] This is most likely due to the occurrence of additional forms of structural disorder, which were not included in the simulations of charge transport. For instance,

fluctuations of the stacking distance, shifting of the dimers out of the stack and geometrical distortions of the hydrogen-bonded dimers will affect the charge carrier mobility.

Based on the calculations discussed above, it can be concluded that the charge carrier mobility along stacks of MOPV dimers can be significantly enhanced by reduction of the twist angle. This can possibly be achieved by modifications in the side chains, which reduce the steric repulsion between them. Alternatively, the introduction of additional functional groups that for instance enable hydrogen bonding in the π-stacking direction can also provide a route to supramolecular aggregates with a more ordered structure.

4.3. *Two-dimensional phenylene-vinylene stacks*

In Section 4.2 the charge transport properties of phenylene-vinylene based materials in solution were considered. Charge transport in oligo(phenylene-vinylene)s has been extensively studied in the solid state also, since these materials are of particular interest for application in LEDs and photovoltaic cells. The charge carrier mobilities in oligo(phenylene-vinylene)s measured in light emitting diodes is generally very low, on the order of $10^{-5}\,cm^2\,V^{-1}\,s^{-1}$.[238] The main reason for this low mobility is the disordered structure. Microwave conductivity experiments have given a direct indication that improved supramolecular order can increase the charge carrier mobility by an order of magnitude.[36]

A possible approach to achieve improved molecular ordering is the synthesis of oligomers and polymers that are not restricted to linear structures, such as two-dimensional conjugated molecules. In such molecules the delocalization of an excess charge is expected to occur in two dimensions. Recently, a new series of two-dimensional conjugated phenylene-vinylene oligomers were synthesized, characterized and evaluated for use in light-emitting diodes.[239,240] These phenylene-vinylene oligomers contain a central phenyl ring, which is substituted with four arms, see Figure 18. The chemical

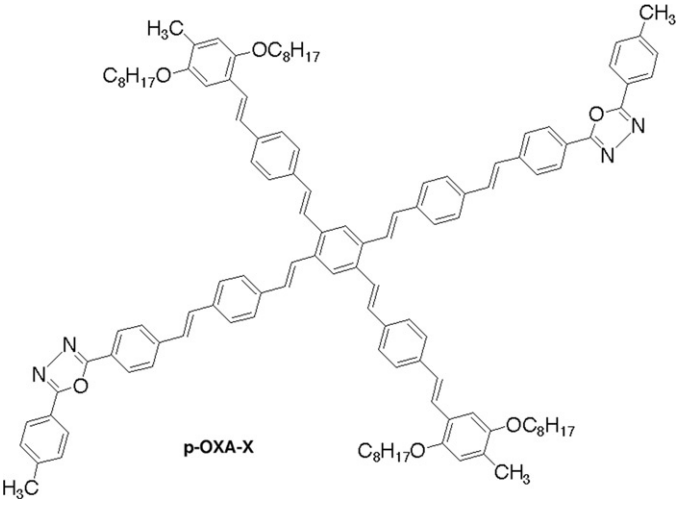

Figure 18. Chemical structure of a two-dimensional phenylene-vinylene, p-OXA-X.

structure of the arms can be varied so that these materials are either p- or n-type semiconductors.[239] Due to their X-shape, these phenylene-vinylene oligomers are called X-mers. Changes in structural symmetry affect the properties of these materials, including absorption and emission spectra, thermal stability, HOMO/LUMO energy levels, tendency to crystallize or to form π stacks in films and device characteristics.[239,240] According to X-ray characterization of powdered samples these X-shaped molecules form π-stacks with an intermolecular distance of 3.5 Å. Hence, these materials have the potential to provide pathways for charge transport along the stacking direction.

In order to gain insight into the charge carrier mobility along these stacks, charge transport calculations have been performed for the X-mer shown in Figure 18.[176] The charge transfer integrals were calculated for different twist angle around the stacking axis, using the FO-procedure described in Section 3. In the calculations the central phenyl rings of the oligomers are superimposed in the stack. This implies that effects of lateral displacements of the X-mers are neglected.

The internal reorganization energies defined in Equation (46) were found to be 0.15 eV and 0.14 eV for the hole and the electron, respectively. These values are smaller than the reorganization energies discussed above for the excess charges on MOPV3 and MOPV4. The smaller values of the reorganization energies for p-OXA-X are consistent with a higher degree of delocalization of the charge over the X-mer in comparison with linear phenylene-vinylenes.

The rate for charge transfer between two p-OXA-X oligomers and the charge carrier mobility of holes and electrons were calculated from Equations (40) and (42), using the values of the effective charge transfer integrals and reorganization energies discussed above. The calculated charge carrier mobility is shown as a function of the twist angle in Figure 19. The calculated hole mobility for p-OXA-X is 34 $cm^2 V^{-1} s^{-1}$ for a twist angle of zero degrees. Increase of the twist angle leads to a strong decrease of the mobility. The electron mobility for zero twist angle is slightly higher than the hole mobility. The electron mobility decreases with the twist angle for angles up to 60 degrees. Interestingly, the electron mobility exhibits a slight increase at larger twist angles.

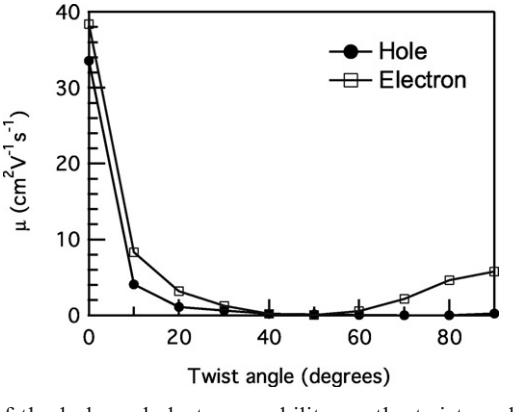

Figure 19. Dependence of the hole and electron mobility on the twist angle for *p*-OXA-X stacks.

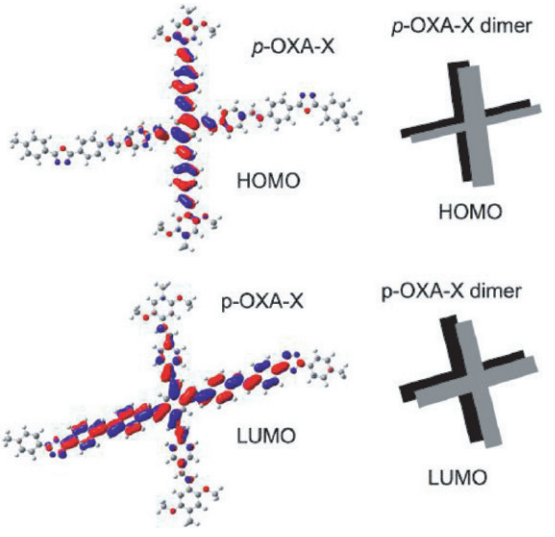

Figure 20. HOMO and LUMO orbitals for the *p*-OXA-Xmer (left side) together with the schematic representation of the HOMO and LUMO orbitals of the *p*-OXA-X dimer (right side).

The difference between the angular dependence of the hole and electron mobility for p-OXA-X can be explained on basis of the spatial distribution of the HOMO and LUMO orbitals. In Figure 20 the HOMO and LUMO orbitals are shown for p-OXA-X together with a schematic representation. The HOMO has the highest density on the phenylene-vinylene arms, while there is hardly any density on the oxadiazole arms. In contrast, for the LUMO the density is almost evenly distributed over the phenylene-vinylene and oxadiazole arms. At a twist angle of zero degrees the charge transfer integral for the HOMOs (LUMOs) of two stacked p-OXA-X oligomers is maximum, due to a strong overlap of the arms of the same nature, see Figure 20. When one p-OXA-X oligomer is rotated over 90 degrees around the stacking axis, the phenylene-vinylene arms on which the positive charge delocalizes have negligible overlap, see Figure 21. As a result, the charge transfer integral and the hole mobility are close to zero. For the electron mobility the situation is different. A rotation of 90 degrees of one p-OXA-X oligomer leads to a situation in which the phenylene-vinylene arms of one X-mer overlap with the arms containing the oxadiazole unit on the other X-mer. Since the density of the LUMO is appreciable on both types of arms the charge transfer integral and the electron mobility do not vanish at 90 degrees.

As discussed above the mobility depends to a large extent on the mutual orientation of the molecules. In order to gain insight into the twist angle between p-OXA-X oligomers in a stack, molecular dynamics simulations were performed. It was found from molecular dynamics simulations that the most favourable conformation occurs at a twist angle of 10 degrees. According to charge transport calculations for a twist angle of 10 degrees and a stacking distance of 3.5 Å the hole mobility is $4.1\,cm^2\,V^{-1}\,s^{-1}$ and the electron mobility is $8.3\,cm^2\,V^{-1}\,s^{-1}$. These calculations involve ordered static molecular stacks. Dynamic structural fluctuations will cause the charge transfer integrals to differ from place to place along the stack. As discussed in Section 4.2 for π-stacked MOPV dimers, the mobility

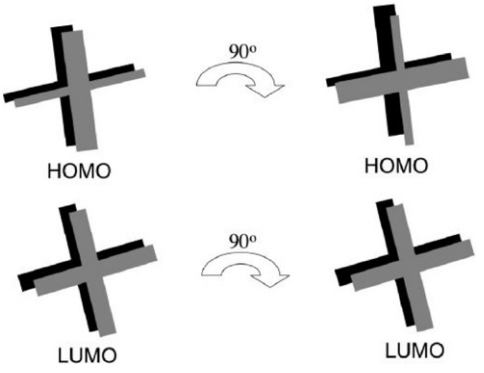

Figure 21. Schematic representation of the HOMO and LUMO orbitals of the *p*-OXA-X dimer explaining the dependence of the charge carrier mobilities on the twist angle.

is determined by the slowest hopping steps, which occur at the largest twist angles. Hence, the mobility of charges on a disordered X-mer stack will be lower than the values obtained for the equilibrium angle of 10 degrees. According to the calculations high charge carrier mobilities can be achieved for stacks of X-mers with small mutual twist angles.

4.4. *DNA*

The efficiency of charge transport in DNA has been a subject of considerable debate over the past two decades. As noted in the introduction, the possibility of electrical conductivity in DNA was put forward for the first time in 1962 by Eley and Spivey who noted the similarity between the structure of DNA and one-dimensional organic crystals.[66] The interest in charge transfer in DNA took a flight in the early 1990s after a series of papers in which it was suggested that ultrafast photoinduced charge transfer takes place over large distances between donors and acceptors that are intercalated in DNA.[241–243] These claims have prompted a wide variety of experimental and theoretical studies into the nature of charge migration through DNA, which is still a subject of intense research.[64,65] Initially, experiments on charge transfer were mostly interpreted in terms of classical theory for charge transfer from a donor via an intervening DNA bridge to an acceptor. In this case the rate of charge transfer depends exponentially on the distance, R, between the donor and the acceptor,

$$k_{CT}(R) = k_0 \exp(-\beta R) \tag{47}$$

where k_0 is a scaling factor and β is the so-called fall-off parameter which determines the distance dependence. The value of β has often been used to distinguish between different mechanisms for charge transport through DNA. A small value for β (≈ 0.1 Å^{-1}) indicates a weak dependence on distance. This can occur when the energy of the charge at the donor is close to that on the intervening bridge and leads to a considerable charge density on the bridge during the charge transfer process.[124] A large β (≈ 1 Å^{-1}) represents strong distance dependence, characteristic of a single-step tunnelling process in which the charge does not actually become localized on the bridge.[123,124,127]

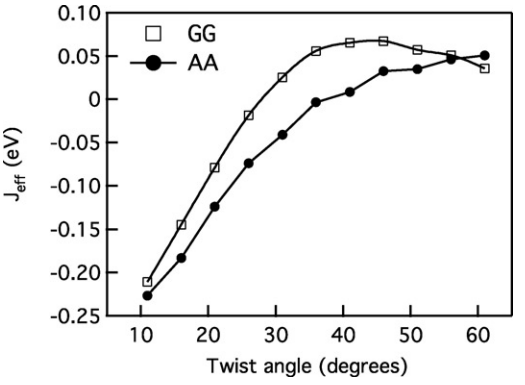

Figure 22. Twist angle dependence of the effective charge transfer integrals for adjacent G and A nucleobases in poly(dG)·poly(dC) and poly(dA)·poly(dT) DNA.

Apart from the study of charge transfer through DNA in donor–DNA–acceptor systems there have also been some direct measurements of charge transport through DNA molecules positioned between electrodes.[244–246] These studies involve measurements of current–voltage characteristics and do not provide information on the value of the mobility of charges in DNA, since the charge carrier density is unknown. In order to estimate the charge carrier mobility in DNA theoretically, the charge transport parameters discussed in Section 3 must be known. The values of the effective charge transfer integrals between neighbouring nucleobases have been calculated previously using the FO-procedure described in Section 3 for all possible combinations of nucleobases.[127] In Figure 22 the effective charge transfer integral for intrastrand charge transfer between guanine (G) and between adenine (A) nucleobases is shown as a function of the twist angle between neighbouring base pairs. Figure 22 shows that the value of J_{eff} is rather small (< 0.1 eV) near the equilibrium twist angle of 36 degrees. It must be noted that fluctuations of the twist angles lead to variations of the charge transfer integral that exceed the value at the equilibrium angle. The charge transfer integrals can be used to describe hole transport along poly(dG)·poly(dC) and poly(dA)·poly(dT) DNA, which consist of only G:C or A:T base pairs, respectively, with all G or A nucleobases within the same strand. Since the ionization energy of G and A is much lower than for cytosine (C) and thymine (T) nucleobases, holes will be almost completely localized on G or A. The mobility of charges along poly(dG)·poly(dC) and poly(dA)·poly(dT) will be much higher than for DNA consisting of both G:C and A:T base pairs. This is due to the fact that for poly(dG)·poly(dC) and poly(dA)·poly(dT) all base pairs, and consequently the site energies, are identical. By contrast, in natural DNA or other sequences containing both G:C and A:T base pairs charge transport occurs via different nucleobases and the variation of the site energies reduces the mobility of holes.

The calculated internal reorganization energy for the DNA nucleobases is close to 0.5 eV.[178] If charge transport in DNA takes place in its natural aqueous environment the external reorganization energy, resulting from reorientation of water molecules around the charge, must also be taken into account. The external or solvent

reorganization energy has been estimated to be 0.69 eV.[247] Combining these two values gives and estimate of the total reorganization energy larger than 1 eV; *i.e.* more than an order of magnitude larger than the effective charge transfer integral. This value of the reorganization energy agrees very well with the value that needed to be invoked to theoretically reproduce experimental values of absolute rates of charge transfer through DNA.[127]

Using the calculated charge transfer integrals and the estimated reorganization energy of 1 eV, the mobility of a hole along poly(dG)·poly(dC) and poly(dA)·poly(dT) was calculated using Equation (42) with the polaronic hopping rate in Equation (40). Disorder in the form of twisting of base pairs, and consequently fluctuations of the charge transfer integrals, was taken into account in these calculations.[127] For a reorganization energy equal to 1 eV the mobility of holes is calculated to be $10^{-4}\,cm^2\,V^{-1}\,s^{-1}$ and $2\times10^{-5}\,cm^2\,V^{-1}\,s^{-1}$ for stacks poly(dG)·poly(dC) and poly(dA)·poly(dT), respectively. A slightly different value of the total reorganization energy equal to 0.63 eV must be used to reproduce the mobility of $9\times10^{-4}\,cm^2\,V^{-1}\,s^{-1}$ for holes on poly(dA)·poly(dT), as reported in reference[248]. More accurate calculations of the mobility require knowledge of the reorganization energy for the specific sequences studied in experiments on the conductance of DNA. Nevertheless the estimated mobility values given above are orders of magnitude smaller than the mobility values of charges in the π-stacked systems discussed in Sections 4.1–4.3. This is mainly due to the much higher reorganization energy for DNA. However, the estimated mobility values for poly(dG)·poly(dC) and poly(dA)·poly(dT) are comparable to those found for structurally disordered polymers in opto-electronic devices.

5. Conclusions

An overview of theoretical frameworks to describe the mobility of charge carriers in organic molecular materials has been discussed. The results of theoretical calculations were used to obtain insights into the factors that govern the mobility of charge carriers along stacks of triphenylene or oligo(phenylene-vinylene) molecules and along DNA strands. Calculated charge transfer integrals and site energies strongly depend on the mutual arrangement of adjacent molecules. Hence, details of the structural organization and dynamics at the molecular level are needed for a quantitative theoretical description of experimental mobility values. For favourable mutual arrangement of triphenylene or oligo(phenylene-vinylene) molecules the calculated charge transfer integrals and reorganization energies are comparable to those for organic molecular crystals such as pentacene. This suggests that a charge carrier mobility well above $1\,cm^2\,V^{-1}\,s^{-1}$, which is typical for organic crystals, can also be achieved for stacks of triphenylenes and oligo(phenylene-vinylene) with suitable structural order. According to calculations the mobility of charge carriers along DNA strands is strongly limited by a high reorganization energy, which largely exceeds the charge transfer integrals.

Acknowledgements

The Netherlands Organisation for Scientific Research (NWO) and The Netherlands Foundation for Fundamental Research on Matter (FOM) are acknowledged for financial support.

References

[1]R.H. Friend, Pure Appl. Chem. **73**, 425 (2001).
[2]A. Moliton, *Optoelectronics of Molecules and Polymers* (Springer, New York, 2006).
[3]T. Blythe and D. Bloor, *Electrical Properties of Polymers* (Cambridge University Press, Cambridge, 2005).
[4]A. Facchetti, Mater. Today **10**, 28 (2007).
[5]Y. Shirota and H. Kageyama, Chem. Rev. **107**, 953 (2007).
[6]J. Zaumseil and H. Sirringhaus, Chem. Rev. **107**, 1296 (2007).
[7]J.G.C. Veinot and T.J. Marks, Acc. Chem. Res. **38**, 632 (2005).
[8]S.E. Gledhill, B. Scott and B.A. Gregg, J. Mater. Res. **20**, 3167 (2005).
[9]H. Hoppe and N.S. Saricifti, J. Mater. Res. **19**, 1924 (2004).
[10]H. Spanggaard and F.C. Krebs, Sol. En. Mat. Sol. Cells **83**, 125 (2004).
[11]S. Gunes, H. Neugebauer and N.S. Saricifti, Chem. Rev. **107**, 1324 (2007).
[12]M.D. Archer and R. Hill (Ed.), *Clean Electricity from Photovoltaics* (Imperial College Press, London, 2001).
[13]J. Nelson, *The Physics of Solar Cells* (Imperial College Press, London, 2003).
[14]C.J. Brabec, V. Dyakonov, J. Parisi, and N.S. Sariciftci (Ed.), *Organic Photovoltaics* (Springer, Heidelberg, 2003).
[15]S. Sun and N.S. Sariciftci, *Organic Photovoltaics* (Taylor & Francis, Boca Raton, 2005).
[16]R. Farchioni and G. Grosso (Ed.), *Organic Electronic Materials* (Springer, Berlin, 2001).
[17]E. Cantatore, T.C.T. Geuns, G.H. Gelinck, E. van Veenendaal, A.F.A. Gruijthuijsen, L. Schrijnemakers, S. Drews and D.M. de Leeuw, IEEE J. Solid St. Circ. **42**, 84 (2007).
[18]J.S. Rasul, Microelectronics Reliability **44**, 135 (2004).
[19]G. Padmanaban and S. Ramakrishnan, J. Am. Chem. Soc. **122**, 2244 (2000).
[20]P.F. van Hutten, V.V. Krasnikov and G. Hadziioannou, Acc. Chem. Res. **32**, 257 (1999).
[21]J. Cornil, D. Beljonne, J.P. Calbert and J.-L. Brédas, Adv. Mater. **13**, 1053 (2001).
[22]C. Reese and Z. Bao, Mater. Today **10**, 20 (2007).
[23]C. Reese, W.J. Chung, M.M. Ling, M. Roberts and Z. Bao, Appl. Phys. Lett. **89**, 202108 (2006).
[24]W.A. Schoonveld, J. Vrijmoeth and T.M. Klapwijk, Appl. Phys. Lett. **73**, 3884 (1998).
[25]O.D. Jurchescu, J. Baas and T.T.M. Palstra, Appl. Phys. Lett. **84**, 3061 (2004).
[26]V. Podzorov, E. Menard, A. Borissov, V. Kiryukhin, J.A. Rogers and M.E. Gershenson, Phys. Rev. Lett. **93**, 086602 (2004).
[27]R.W.I. de Boer, M.E. Gershenson, A.F. Morpurgo and V. Podzorov, Phys. Ptat. Sol. (a) **201**, 1302 (2004).
[28]R. Zeis, T. Siegrist and C. Kloc, Appl. Phys. Lett. **86**, 022103 (2005).
[29]G. Horowitz, F. Garnier, A. Yassar, R. Hajlaoui and F. Kouki, Adv. Mater. **8**, 52 (1996).
[30]M. Ichikawa, H. Yanagi, Y. Shimizu, S. Hotta, N. Suganuma, T. Koyama and Y. Taniguchi, Adv. Mater. **14**, 1272 (2002).
[31]R. Zeis, C. Kloc, K. Takimiya, Y. Kunugi, Y. Konda, N. Niihara and T. Otsubo, Jap. J. Appl. Phys. **44**, 3712 (2005).
[32]D.Y. Godovsky, Adv. Pol. Sci. **153**, 163 (2000).
[33]J. Bharathan and Y. Yang, Appl. Phys. Lett. **72**, 2660 (1998).
[34]H. Sirringhaus, T. Kawase, R.H. Friend, T. Shimoda, M. Inbasekaran, W. Wu and E.P. Woo, Science **290**, 2123 (2000).
[35]H. Sirringhaus, P.J. Brown, R.H. Friend, M.M. Nielsen, K. Bechgaard, B.M.W. Langeveld-Voss, A.J.H. Spiering, R.A.J. Janssen, E.W. Meijer, P. Herwig and D.M. de Leeuw, Nature **401**, 685 (1999).
[36]J.M. Warman, G.H. Gelinck and M.P. de Haas, J. Phys. C. **14**, 9935 (2002).

[37]P. Prins, F.C. Grozema, J.M. Schins, S. Patil, U. Scherf and L.D.A. Siebbeles, Phys. Rev. Lett. **96**, 146601 (2006).
[38]M.D. Newton, Chem. Rev. **91**, 767 (1991).
[39]J.E. Anthony, Chem. Rev. **106**, 5028 (2006).
[40]G. Horowitz, B. Bachet, A. Yassar, P. Lang, F. Demanze, J.-L. Fave and G. Garnier, Chem. Mater. **7**, 1337 (1995).
[41]J.-M. Lehn, Rep. Prog. Phys. **67**, 249 (2004).
[42]J.A.A.W. Elemans, A.E. Rowan and R.J.M. Nolte, J. Mater. Chem. **13**, 2661 (2003).
[43]P. Leclère, M. Surin, P. Jonkheijm, O. Henze, A.P.H.J. Schenning, F. Biscarini, A.C. Grimsdale, W.J. Feast, E.W. Meijer, K. Müllen, J.-L. Brédas and R. Lazzaroni, Eur. Pol. J. **40**, 885 (2004).
[44]F.J.M. Hoeben, P. Jonkheijm, E.W. Meijer and A.P.H.J. Schenning, Chem. Rev. **105**, 1491 (2005).
[45]B. Wegewijs, M.P. de Haas, D.M. de Leeuw, R. Wilson and H. Sirringhaus, Synth. Met. **101**, 534 (1999).
[46]F.C. Grozema, B.R. Wegewijs, M.P. de Haas, L.D.A. Siebbeles, D.M. de Leeuw, R. Wilson and H. Sirringhaus, Synth. Met. **119**, 463 (2000).
[47]J.F. van der Pol, E. Neeleman, J.W. Zwikker, R.J.M. Nolte, W. Drenth, J. Aerts, R. Visser and S.J. Picken, Liq. Cryst. **6**, 577 (1989).
[48]N. Kobayashi, Cord. Chem. Rev. **219**, 99 (2001).
[49]C.D. Simpson, J. Wu, M.D. Watson and K. Müllen, J. Mater. Chem. **14**, 494 (2004).
[50]J.M. Warman and A.M. van de Craats, Mol. Cryst. Liq. Cryst. **396**, 41 (2003).
[51]J.M. Warman, M.P. de Haas, G. Dicker, F.C. Grozema, J. Piris and M.G. Debije, Chem. Mat. **16**, 4600 (2004).
[52]J.S. Wu, W. Pisula and K. Mullen, Chem. Rev. **107**, 718 (2007).
[53]S. Laschat, A. Baro, N. Steinke, F. Giesselmann, C. Hagele, G. Scalia, R. Judele, E. Kapatsina, S. Sauer, A. Schreivogel and M. Tosoni, Angew. Chem. Int. Ed. **46**, 4832 (2007).
[54]Z. An, J. Yu, S.C. Jones, S. Barlow, S. Yoo, B. Domercq, P. Prins, L.D.A. Siebbeles, B. Kippelen and S.J. Marder, Adv. Mater. **17**, 2580 (2005).
[55]Z. Chen, V. Stepanenko, V. Dehm, P. Prins, L.D.A. Siebbeles, J. Seibt, P. Marquetand, V. Engel and F. Würthner, Chem. Eur. J. **13**, 436 (2007).
[56]V. Dehm, Z. Chen, U. Baumeister, P. Prins, L.D.A. Siebbeles and F. Würthner, Org. Lett. **9**, 1085 (2007).
[57]A.M. van de Craats, N. Stutzmann, O. Bunk, M.M. Nielsen, M. Watson, K. Müllen, H.D. Chanzy, H. Sirringhaus and R.H. Friend, Adv. Mater. **15**, 495 (2003).
[58]I.O. Shklyarevskiy, P. Jonkheijm, N. Stutzmann, D. Wasserberg, H.J. Wondergem, P.C.M. Christianen, A.P.H.J. Schenning, D.M. de Leeuw, Z. Tomovic, J.S. Wu, K. Mullen and J.C. Maan, J. Am. Chem. Soc. **127**, 16233 (2005).
[59]A.M. van de Craats, J.M. Warman, A. Fechtenkotter, J.D. Brand, M.A. Harbison and K. Mullen, Adv. Mater. **11**, 1469 (1999).
[60]Q. Zhang, P. Prins, S.C. Jones, S. Barlow, T.K. Kondo, Z. An, L.D.A. Siebbeles and S.J. Marder, Org. Lett. **7**, 5019 (2005).
[61]I. Paraschiv, M. Giesbers, B. van Lagen, F.C. Grozema, R.D. Abellon, L.D.A. Siebbeles, A.T.M. Marcelis, H. Zuilhof and E.J.R. Sudhölter, Chem. Mater. **18**, 968 (2006).
[62]F.S. Schoonbeek, J.H. Van Esch, B.R. Wegewijs, D.B.A. Rep, M.P. de Haas, T.M. Klapwijk, R.M. Kellog and B.L. Feringa, Angew. Chem. Int. Ed. **38**, 1393 (1999).
[63]G.B. Schuster (Ed.), *Long-range Charge Transfer in DNA* (Springer-Verlag, Berlin, 2004).
[64]H.-A. Wagenknecht (Ed.), *Charge Transfer in DNA* (Wiley-VCH, Weinheim, 2005).
[65]T. Chakraborty (Ed.), *Charge Migration in DNA* (Springer, Berlin, 2007).
[66]D.D. Eley and D.I. Spivey, Trans. Faraday Soc. **58**, 411 (1962).
[67]J.D. Watson and F.H.C. Crick, Nature **171**, 737 (1953).
[68]R.G. Endres, D.L. Cox and R.R.P. Singh, Rev. Mod. Phys. **76**, 195 (2004).

[69]M. Dressel and G. Grüner, *Electrodynamics of Solids* (Cambridge University Press, Cambridge, 2002).
[70]G. Grosso and G.P. Parravicini, *Solid State Physics* (Academic Press, London, 2000).
[71]J. Callaway, *Quantum Theory of the Solid State* (Academic Press, London, 1991).
[72]R. Kubo, J. Phys. Soc. Japan **12**, 570 (1957).
[73]G.D. Mahan, *Many-Particle Physics* (Plenum, New York, 1981).
[74]G.D. Mahan, Phys. Rep. **145**, 251 (1987).
[75]H. Scher and M. Lax, Phys. Rev. B **7**, 4491 (1973).
[76]J.C. Dyre and T.B. Schroder, Rev. Mod. Phys. **72**, 873 (2000).
[77]U. Mizutani, *Introduction to the Electron Theory of Metals* (Cambridge University Press, Cambridge, 2001).
[78]D.N. Zubarev, *Nonequilibrum Statistical Thermodynamics* (Plenum Press, New York, 1974).
[79]E.A. Silinsh, *Organic Molecular Crystals* (Springer-Verlag, Berlin, 1980).
[80]M. Pope and C.E. Swenberg, *Electronic Processes in Organic Crystals* (Oxford University Press, Oxford, 1982).
[81]V. Coropceanu, J. Cornil, D.A. da Silva Filho, Y. Olivier, R.J. Silbey and J.L. Brédas, Chem. Rev. **107**, 926 (2007).
[82]P. Prins, F.C. Grozema and L.D.A. Siebbeles, Mol. Sim. **32**, 695 (2006).
[83]J.M. Schins, P. Prins, F.C. Grozema, R.D. Abellon, M.P. de Haas and L.D.A. Siebbeles, Rev. Sci. Instr. **76**, 084703 (2005).
[84]P. Prins, F.C. Grozema, J.M. Schins, T.J. Savenije, S. Patil, U. Scherf and L.D.A. Siebbeles, Phys. Rev. B **73**, 045204 (2006).
[85]P. Prins, F.C. Grozema and L.D.A. Siebbeles, J. Phys. Chem. B **110**, 14659 (2006).
[86]E. Hendry, M. Koeberg, J.M. Schins, L.D.A. Siebbeles and M. Bonn, Phys. Rev. B **70**, 033202 (2004).
[87]E. Hendry, M. Koeberg, J.M. Schins, L.D.A. Siebbeles and M. Bonn, Chem. Phys. Lett. **432**, 441 (2006).
[88]E. Hendry, J.M. Schins, L.P. Candeias, L.D.A. Siebbeles and M. Bonn, Phys. Rev. Lett. **92**, 196601 (2004).
[89]G. Lanzani (Ed.), *Photophysics of Molecuar Materials* (Wiley-VCH, Weinheim, 2006).
[90]C. Kittel, *Introduction to Solid State Physics* (John Wiley, Hoboken, 2005).
[91]J.M. André, J. Delhalle and J.L. Brédas, *Quantum Chemistry Aided Design of Organic Polymers* (World Scientific, Singapore, 1991).
[92]E.F. Valeev, V. Coropceanu, D.A. da Silva, S. Salman and J.L. Brédas, J. Am. Chem. Soc. **128**, 9882 (2006).
[93]K. Senthilkumar, F.C. Grozema, F.M. Bickelhaupt and L.D.A. Siebbeles, J. Chem. Phys. **119**, 9809 (2003).
[94]M. Dressel and M. Scheffer, Ann. Phys. **15**, 535 (2006).
[95]M. Lundstrom, *Fundamentals of Carrier Transport* (Cambridge University Press, Cambridge, 2000).
[96]P. Prins, F.C. Grozema, F. Galbrecht, U. Scherf and L.D.A. Siebbeles, J. Phys. Chem. C **111**, 11104 (2007).
[97]T. Holstein, Ann. Phys. **8**, 343 (1959).
[98]R. Silbey, J. Jortner, S.A. Rice and M.T. Vala, J. Chem. Phys. **42**, 733 (1965).
[99]B. Movaghar, J. Mol. El. **3**, 183 (1987).
[100]A.S. Alexandrov and N. Mott, *Polarons and Bipolarons* (World Scientific, Singapore, 1995).
[101]K. Hannewald, V.M. Stojanovic, J.M.T. Schellekens, P.A. Bobbert, G. Kresse and J. Hafner, Phys. Rev. B **69**, 075211 (2004).
[102]K. Hannewald, V.M. Stojanovic and P.A. Bobbert, J. Phys. C **16**, 2023 (2004).
[103]K. Hannewald and P.A. Bobbert, Appl. Phys. Lett. **85**, 1535 (2004).
[104]N.V. Smith, Phys. Rev. B **64**, 155106 (2001).

[105]G.C. Schatz and M.A. Ratner, *Quantum Mechanics in Chemistry* (Dover Publications, Mineola, NY, 2002).
[106]P. Reineker, Z. Physik **261**, 187 (1973).
[107]D.H. Dunlap and V.M. Kenkre, *Exciton Dynamics in Molecular Crystals and Aggregates* (Springer, Berlin, 1982).
[108]V. May and O. Kühn, *Charge and Energy Transfer Dynamics in Molecular Systems* (Wiley, Berlin, 2000).
[109]W.P. Su, J.R. Schrieffer and A.J. Heeger, Phys. Rev. B **22**, 2099 (1980).
[110]A.J. Heeger, S. Kivelson, J.R. Schrieffer and W.P. Su, Rev. Mod. Phys. **60**, 781 (1988).
[111]H.W. Streitwolf, Phys. Rev. B **58**, 14356 (1998).
[112]Z. An, C.Q. Wu and X. Sun, Phys. Rev. Lett. **93**, 216407 (2004).
[113]S. Stafstrom and A. Johansson, Phys. Rev. Lett. **86**, 3602 (2001).
[114]S. Stafstrom and A. Johansson, Phys. Rev. B **68**, 035206 (2003).
[115]L. Gisslen, A. Johansson and S. Stafstrom, J. Chem. Phys. **121**, 1601 (2004).
[116]M. Hultell and S. Stafstrom, Phys. Rev. B **75**, 104304 (2007).
[117]A. Troisi, Mol. Sim. **32**, 707 (2006).
[118]A. Troisi and G. Orlandi, J. Phys. Chem. A **110**, 4065 (2006).
[119]A. Troisi and G. Orlandi, Phys. Rev. Lett. **96**, 086601 (2006).
[120]R. Kosloff, J. Phys. Chem. **92**, 2087 (1988).
[121]F.C. Grozema, P.T. van Duijnen, Y.A. Berlin, M.A. Ratner and L.D.A. Siebbeles, J. Phys. Chem. B **106**, 7791 (2002).
[122]L.D.A. Siebbeles, F.C. Grozema, M.P. de Haas and J.M. Warman, Rad. Phys. Chem. **72**, 85 (2005).
[123]F.C. Grozema, Y.A. Berlin and L.D.A. Siebbeles, Int. J. Quantum Chem. **75**, 1009 (1999).
[124]F.C. Grozema, Y.A. Berlin and L.D.A. Siebbeles, J. Am. Chem. Soc. **122**, 10903 (2000).
[125]Y.A. Berlin, A.L. Burin, L.D.A. Siebbeles and M.A. Ratner, J. Phys. Chem. A **105**, 5666 (2001).
[126]F.C. Grozema, L.D.A. Siebbeles, Y.A. Berlin and M.A. Ratner, Chem. Phys. Chem **6**, 536 (2002).
[127]K. Senthilkumar, F.C. Grozema, C.F. Guerra, F.M. Bickelhaupt, F.D. Lewis, Y.A. Berlin, M.A. Ratner and L.D.A. Siebbeles, J. Am. Chem. Soc. **127**, 148094 (2005).
[128]V.M. Kenkre and P. Reineker (Ed.), *Exciton Dynamics in Molecuar Crystals and Aggregates* (Springer, Berlin, 1982).
[129]H. Haken and P. Reineker, Z. Physik **249**, 253 (1972).
[130]K. Kitahara and J.W. Haus, Z. Physik B **32**, 419 (1979).
[131]M.A. Palenberg, R.J. Silbey, M. Malagoli and J.L. Brédas, J. Chem. Phys. **112**, 1541 (2000).
[132]M.A. Palenberg, R.J. Silbey and W. Pfluegl, Phys. Rev. B **62**, 3744 (2000).
[133]W. Pfluegl, M.A. Palenberg and R.J. Silbey, J. Chem. Phys. **113**, 5632 (2000).
[134]D.S. Pearson, P.A. Pincus, G.W. Heffner and S.J. Dahman, Macromolecules **26**, 1570 (1993).
[135]P. Prins, F.C. Grozema, J.M. Schins and L.D.A. Siebbeles, Phys. Stat. Sol. (b) **243**, 382 (2006).
[136]M. Jaiswal and R. Menon, Polymer Int. **55**, 1371 (2006).
[137]F. Laquai, G. Wegner and H. Bässler, Phil. Trans. Roy. Soc. **365**, 1473 (2007).
[138]A. Miller and E. Abrahams, Phys. Rev. **120**, 745 (1960).
[139]N.F. Mott, Proc. Roy. Soc. (London) **A126**, 259 (1930).
[140]B.I. Shklovskii and A.L. Efros, *Electronic Properties of Doped Semiconductors* (Springer-Verlag, Berlin, 1984).
[141]D. Emin, Phys. Rev. Lett. **32**, 303 (1974).
[142]N.F. Mott and E.A. Davis, *Electronic Processes in Non-Crystalline Materials* (Clarendon Press, Oxford, 1979).
[143]R.A. Marcus, Ann. Rev. Phys. Chem. **15**, 155 (1964).
[144]D. Emin, Adv. Phys. **24**, 305 (1975).
[145]J. Jortner, J. Chem. Phys. **64**, 4860 (1976).

[146]J. Bixon and J. Jortner, in *Advances in Chemical Physics* edited by I. Prigogine and S.A. Rice (Wiley, New York, 1999).
[147]H. Bässler, Phys. Stat. Sol. b **175**, 15 (1993).
[148]W.F. Pasveer, J. Cottaar, C. Tanase, R. Coehoorn, P.A. Bobbert, P.W.M. Blom, D.M. de Leeuw and M.A.J. Michels, Phys. Rev. Lett. **94**, 206601 (2005).
[149]R. Coehoorn, W.F. Pasveer, P.A. Bobbert and M.A.J. Michels, Phys. Rev. B **72**, 155206 (2005).
[150]Y.N. Gartstein and E.M. Conwell, Chem. Phys. Lett. **245**, 351 (1995).
[151]D.H. Dunlap, P.E. Parris and V.M. Kenkre, Phys. Rev. Lett. **77**, 542 (1996).
[152]B. Movaghar, J. Mol. El. **4**, 79 (1988).
[153]I.I. Fishchuk, Phil. Mag. B **81**, 561 (2001).
[154]O. Hilt and L.D.A. Siebbeles, Chem. Phys. **229**, 257 (1998).
[155]P.K. Watkins, A.B. Walker and G.L.B. Verschoor, Nanoletters **5**, 1814 (2005).
[156]S.J. Martin, A. Kambili and A.B. Walker, Phys. Rev. B **67**, 165214 (2003).
[157]A.B. Walker, A. Kambili and S.J. Martin, J. Phys. C **14**, 9825 (2002).
[158]T. Kreouzis, D. Poplavskyy, S.M. Tuladhar, M. Campoy-Quiles, J. Nelson, A.J. Campbell and D.D.C. Bradley, Phys. Rev. B **73**, 235201 (2006).
[159]J.M. Frost, C.F.S.M. Tuladhar and J. Nelson, Nanoletters **6**, 1674 (2006).
[160]Y. Olivier, V. lemaur, J.L. Brédas and J. Cornil, J. Phys. Chem. A **110**, 6356 (2006).
[161]A.J. Chatten, S.M. Tuladhar, S.A. Choulis, D.D.C. Bradley and J. Nelson, J. Mat. Sci. **40**, 1393 (2005).
[162]S. Athanasopoulos, J. Kirkpatrick, D. Martinez, J.M. Frost, C.M. Foden, A.B. Walker and J. Nelson, Nanoletters **7**, 1785 (2007).
[163]V. Lemaur, D.A. da Silva Filho, V. Coropceanu, M. Lehmann, Y. Geerts, J. Piris, M.G. Debije, A.M. van de Craats, K. Senthilkumar, L.D.A. Siebbeles, J.M. Warman, J.L. Brédas and J. Cornil, J. Am. Chem. Soc. **126**, 3271 (2004).
[164]P. Prins, K. Senthilkumar, F.C. Grozema, P. Jonkheijm, A.P.H.J. Schenning, E.W. Meijer and L.D.A. Siebbeles, J. Phys. Chem. B **109**, 18267 (2005).
[165]J. Kirkpatrick, V. Marcon, J. Nelson, K. Kremer and D. Andrienko, Phys. Rev. Lett. **98**, 227402 (2007).
[166]Y.A. Berlin and A.L. Burin, Chem. Phys. Lett. **257**, 665 (1996).
[167]L.D.A. Siebbeles and Y.A. Berlin, Chem. Phys. Lett. **265**, 460 (1997).
[168]O. Hilt and L.D.A. Siebbeles, Chem. Phys. Lett. **269**, 257 (1997).
[169]Y.A. Berlin, L.D.A. Siebbeles and A.A. Zharikov, Chem. Phys. Lett. **276**, 361 (1997).
[170]A.M. van de Craats, L.D.A. Siebbeles, I. Bleyl, D. Haarer, Y.A. Berlin, A.A. Zharikov and J.M. Warman, J. Phys. Chem. B **102**, 9625 (1998).
[171]Y.A. Berlin and L.D.A. Siebbeles, Chem. Phys. Lett. **291**, 85 (1998).
[172]K. Senthilkumar, F.C. Grozema, C.F. Guerra, F.M. Bickelhaupt and L.D.A. Siebbeles, J. Am. Chem. Soc. **126**, 3271 (2003).
[173]A. Szabo and N.S. Ostlund, *Modern Quantum Chemistry* (Dover, New York, 1996).
[174]J. Huang and M. Kertesz, J. Chem. Phys. **122**, 234707 (2005).
[175]G. Te Velde, F.M. Bickelhaupt, E.J. Baerends, C. Fonseca Guerra, S.J.A. Van Gisbergen, J.G. Snijders and T. Ziegler, J. Comp. Chem. **22**, 931 (2001).
[176]S. Fratiloiu, K. Senthilkumar, F.C. Grozema, H. Christian-Pandya, Z.I. Niazimbetova, Y.J. Bhandari, M.E. Galvin and L.D.A. Siebbeles, Chem. Mater. **18**, 2118 (2006).
[177]L. Eijck, K. Senthilkumar, L.D.A. Siebbeles and G.J. Kearley, Physica B **350**, 220 (2004).
[178]J. Olofsson and S. Larsson, J. Phys. Chem. B **105**, 10398 (2001).
[179]A.A. Voityuk, N. Rösch, M. Bixon and J. Jortner, J. Phys. Chem. **104**, 9740 (2000).
[180]A.A. Voityuk, J. Jortner, J. Bixon and N.J. Rosch, J. Chem. Phys. **114**, 5614 (2001).
[181]A.A. Voityuk and N.J. Rosch, Chem. Phys. **117**, 5607 (2002).
[182]P.F. Barbara, T.J. Meyer and M.A. Ratner, J. Phys. Chem. **100**, 13148 (1996).
[183]J.L. Brédas, D. Beljonne, V. Coropceanu and J. Cornil, Chem. Rev. **104**, 4971 (2004).

[184]J.C. Sancho-Garcia, Chem. Phys. **331**, 321 (2007).
[185]S. Chandrasekhar and S. Krishna Prasad, Contemp. Phys. **40**, 237 (1999).
[186]R.J. Bushby and O.R. Lozman, Curr. Opinion Sol. State Mat. Sci. **6**, 569 (2002).
[187]R.J. Bushby and O.R. Lozman, Curr. Opi. Coll. Int. Sci. **7**, 343 (2002).
[188]S. Kumar, Liq. Cryst. **31**, 1037 (2004).
[189]A.M. Levelut, J. Physique **40**, L81 (1979).
[190]E. Fontes, P.A. Heiney and W.H. de Jeu, Phys. Rev. Lett. **61**, 1202 (1988).
[191]P.A. Heiney, E. Fontes, W.H. de Jeu, A. Riera, P. Carroll and A.B. Smith, J. Phys. France **50**, 461 (1989).
[192]S.H.J. Idziak, P.A. Heiney, J.P. McCauley, P. Carroll and A.B. Smith, Mol. Cryst. Liq. Cryst. **237**, 271 (1993).
[193]X. Shen, R.Y. Dong, N. Boden, R.J. Bushby, P.S. Martin and A. Wood, J. Chem. Phys. **108**, 4324 (1998).
[194]F.M. Mulder, J. Stride, S.J. Picken, P.H.J. Kouwer, M.P. de Haas, L.D.A. Siebbeles and G.J. Kearley, J. Am. Chem. Soc. **125**, 3860 (2003).
[195]S. Krishna Prasad, D.S. Shankar Rao, S. Chandrasekhar and S. Kumar, Mol. Cryst. Liq. Cryst. **396**, 121 (2003).
[196]J. Zhang and R.Y. Dong, J. Phys. Chem. B **110**, 15075 (2006).
[197]G. Cinacchi, R. Colle and A. Tani, J. Phys. Chem. B **108**, 7969 (2004).
[198]O. Kruglova, F.M. Mulder, L.D.A. Siebbeles and G.J. Kearley, Chem. Phys. **330**, 333 (2006).
[199]L. Muccioli, R. Berardi, S. Orlandi, M. Ricci and C. Zannoni, Theor. Chem. Acc. **117**, 1085 (2007).
[200]J.M. Warman, M.P. de Haas, K.J. Smit, M.N. Paddon-Row and J.F. van der Pol, Mol. Cryst. Liq. Cryst. **183**, 375 (1990).
[201]N. Boden, R.J. Bushby, A.N. Cammidge, J. Clements, R. Luo and K.J. Donovan, Mol. Cryst. Liq. Cryst. **261**, 251 (1995).
[202]N. Boden, R.J. Bushby and J. Clements, J. Chem. Phys. **98**, 5920 (1993).
[203]D. Adam, F. Closs, T. Frey, D. Funhoff, D. Haarer, H. Ringsdorf, P. Schuhmacher and K. Siemensmeyer, Phys. Rev. Lett. **70**, 457 (1993).
[204]D. Adam, D. Haarer, F. Closs, T. Frey, D. Funhoff, K. Siemensmeyer, P. Schuhmacher and H. Ringsdorf, Ber. Bunsenges. Phys. Chem. **97**, 1366 (1993).
[205]D. Adam, P. Schuhmacher, J. Simmerer, L. Haussling, K. Siemensmeyer, K.H. Etzbach, H. Ringsdorf and D. Haarer, Nature **371**, 141 (1994).
[206]D. Adam, P. Schuhmacher, J. Simmerer, L. Haussling, W. Paulus, K. Siemensmeyer, K.H. Etzbach, H.H. Ringsdorf and D. Haarer, Adv. Mater. **7**, 276 (1995).
[207]H. Bengs, F. Closs, T. Frey, D. Funhoff, H. Ringsdorf and K. Siemensmeyer, Mol. Cryst. Liq. Cryst. **15**, 565 (1993).
[208]N. Boden, R.J. Bushby, J. Clements, K.J. Donovan, B. Movaghar and T. Kreouzis, Phys. Rev. B **58**, 3063 (1998).
[209]A. Ochse, A. Kettner, J. Kopitzke, J.H. Wendorff and H. Bässler, Phys. Chem. Chem. Phys. **1**, 1757 (1999).
[210]T. Kreouzis, K. Scott, K.J. Donovan, N. Boden, R.J. Bushby, O.R. Lozman and Q. Liu, Chem. Phys. **262**, 489 (2000).
[211]T. Kreouzis, K.J. Donovan, N. Boden, R.J. Bushby, O.R. Lozman and Q. Liu, J. Chem. Phys. **114**, 1797 (2001).
[212]R.J. Bushby, K.J. Donovan, T. Kreouzis and O.R. Lozman, Opto-Electronics Rev. **13**, 269 (2005).
[213]H. Lino, J. Hanna and D. Haarer, Phys. Rev. B **72**, 193203 (2005).
[214]H. Lino, J. Hanna and D. Haarer, Mol. Cryst. Liq. Cryst. **436**, 1171 (2005).

[215]H. Lino, Y. Takayashiki, J. Hanna, R.J. Bushby and D. Haarer, Appl. Phys. Lett. **87**, 192105 (2005).
[216]J.M. Warman and P.G. Schouten, J. Phys. Chem. **99**, 17181 (1995).
[217]A.M. van de Craats, J.M. Warman, M.P. de Haas, D. Adam, J. Simmerer, D. Haarer and P. Schuhmacher, Adv. Mater. **8**, 823 (1996).
[218]A.M. van de Craats, M.P. de Haas and J.M. Warman, Synth. Met. **86**, 2125 (1997).
[219]A.M. van de Craats, P.G. Schouten, J.M. Warman and J. Jap., Liq. Cryst. Soc. **2**, 12 (1998).
[220]A.M. van de Craats and J.M. Warman, Adv. Mater. **13**, 130 (2001).
[221]B.R. Wegewijs, L.D.A. Siebbeles, N. Boden, R.J. Bushby, B. Movaghar, O.R. Lozman, Q. Liu, A. Pecchia and L.A. Mason, Phys. Rev. B **65**, 245112 (2002).
[222]M.J. Arikainen, N. Boden, R.J. Bushby, J. Clements, B. Movaghar and A. Wood, J. Mater. Chem. **5**, 2161 (1995).
[223]N. Boden, R.J. Bushby, J. Clements, B. Movaghar, K.J. Donovan and T. Kreouzis, Phys. Rev. B **52**, 13274 (1995).
[224]L.J. Lever, R.W. Kelsall and R.J. Bushby, Phys. Rev. B **72**, 035130-1 (2005).
[225]J. Cornil, V. Lemaur, J.P. Calbert and J.L. Brédas, Adv. Mater. **14**, 726 (2002).
[226]A. Pecchia, O.R. Lozman, B. Movaghar, N. Boden, R.J. Bushby, K.J. Donovan and T. Kreouzis, Phys. Rev. B **65**, 104204 (2002).
[227]R.C. Weast, *Handbook of Chemistry and Physics* (CRC Press, Cleveland Ohio, 1985–1986).
[228]W. Deng and W.A. Goddard III, J. Phys. Chem. B **108**, 8641 (2004).
[229]L.M. Herz, C. Daniel, C. Silva, F.J.M. Hoeben, A.P.H.J. Schenning, E.W. Meijer, R.H. Friend and R.T. Phillips, Phys. Rev. B **68**, 045203 (2003).
[230]D. Beljonne, E. Hennebicq, C. Daniel, L.M. Herz, C. Silva, G.D. Scholes, F.J.M. Hoeben, P. Jonkheijm, A.P.H.J. Schenning, S.C.J. Meskers, R.T. Phillips, R.H. Friend and E.W. Meijer, J. Phys. Chem. B **109**, 10594 (2005).
[231]M. Durkut, M. Mas-Torrent, P. Hadley, P. Jonkheijm, A.P.H.J. Schenning, E.W. Meijer, S. George and A. Ajayaghosh, J. Chem. Phys. **124**, 154704 (2006).
[232]P. Jonkheim, F.J.M. Hoeben, R. Kleppinger, J. Van Herrikhuyzen, A.P.H.J. Schenning and E.W. Meijer, J. Am. Chem. Soc. **125**, 15941 (2003).
[233]C.R.L.P. Jeukens, P. Jonkheijm, F.J.P. Wijnen, J.C. Gielen, P.C.M. Christianen, A.P.H.J. Schenning, E.W. Meijer and J.C. Maan, J. Am. Chem. Soc. **127**, 8280 (2005).
[234]R.J.O.M. Hoofman, M.P. de Haas, L.D.A. Siebbeles and J.M. Warman, Nature **392**, 54 (1998).
[235]F.C. Grozema, L.D.A. Siebbeles, J.M. Warman, S. Seki, S. Tagawa and U. Scherf, Adv. Mater. **14**, 228 (2002).
[236]F.C. Grozema, R.J.O.M. Hoofman, L.P. Candeias, M.P. de Haas, J.M. Warman and L.D.A. Siebbeles, J. Phys. Chem. A **107**, 5976 (2003).
[237]F.C. Grozema, L.P. Candeias, M. Swart, P.T. van Duijnen, J. Wildeman, G. Hadziioannou, L.D.A. Siebbeles and J.M. Warman, J. Chem. Phys. **117**, 11366 (2002).
[238]P.W.M. Blom and M.C.J.M. Vissenberg, Mater. Sci. Eng. **27**, 53 (2000).
[239]Z.I. Niazimbetova, H.Y. Christian, Y.J. Bhandari, F.L. Beyer and M.E. Galvin, J. Phys. Chem. B **108**, 8673 (2004).
[240]H.K. Cristian-Pandya, Z.I. Niazimbetova, F.L. Beyer and M.E. Galvin, Chem. Mater. **19**, 993 (2007).
[241]C.J. Murphy, M.R. Arkin, Y. Jenkins, N.D. Gathlia, S.H. Bossmann, N.J. Turro and J.K. Barton, Science **262**, 1025 (1993).
[242]M.R. Arkin, E.D.A. Stemp, R.E. Holmlin, J.K. Barton, A. Hormann, E.J.C. Olson and P.F. Barbara, Science **273**, 475 (1996).
[243]C.J. Murphy, M.R. Arkin, N.D. Ghatlia, S.H. Bossmann, N.J. Turro and J.K. Barton, Proc. Nat. Acad. Sci. **91**, 5315 (1994).

[244]D. Porath, A. Bezryadin, S. de Vries and C. Dekker, Nature **403**, 635 (2000).
[245]P.J. De Pablo, F. Moreno-Herrero, J. Colchero, J. Gómez Herrero, P. Herrero, A.M. Baró, P. Ordejón, J.M. Soler and E. Artacho, Phys. Rev. Lett. **85**, 4992 (2000).
[246]A.J. Storm, J. Van Noort, S. de Vries and C. Dekker, Appl. Phys. Lett. **79**, 3881 (2001).
[247]D.N. LeBard, M. Lilichenko, D.V. Matyushov, Y.A. Berlin and M.A. Ratner, J. Phys. Chem. B **107**, 14509 (2003).
[248]T. Takada, T. Kawai, X. Cai, A. Sugimoto, M. Fujitsuka and T. Majima, J. Am. Chem. Soc. **126**, 1125 (2004).